

Design, Analysis, Assembly, and Test of a High-Powered Model Rocket

A Major Qualifying Report

Submitted to the Faculty of the

WORCESTER POLYTECHNIC INSTITUTE

In Partial Fulfillment of the Requirements for the

Degree of Bachelor of Science

In Aerospace Engineering

By



Nathan Brumble



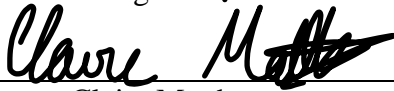
Robert Doyle



Abigail Duval



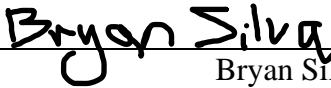
Melissa Kelly



Claire Matthews



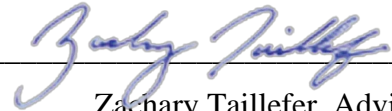
Cameron McAfee



Bryan Silva

March 1, 2024

Approved by:



Zachary Taillefer, Advisor

Professor, Aerospace Engineering

Department

WPI

This report represents the work of one or more WPI undergraduate students submitted to the faculty as evidence of completion of a degree requirement. WPI routinely publishes these reports on the web without editorial or peer review.

## Abstract

This report details the development of a high-powered model rocket capable of reaching an altitude of 1500 feet. The Airframe and Recovery Systems (ARS), Flight Dynamics and Analysis (FDA), and Propulsion, Thermal, and Separation System (PTSS) subgroups designed, modeled, and analyzed the completed project pre- and post-flight. The ARS subgroup designed, fabricated, and assembled the overall mechanical structure and integration of other subsystems. The FDA subgroup analyzed the aerodynamic loads on the vehicle during flight, selected, simulated, and integrated various sensors for flight and vehicle dynamics, and analyzed and simulated the rocket's performance. The PTSS subgroup selected, modeled, and tested the rocket motor and analyzed the thermal loads from the motor during flight. All subgroups worked in coordination to completely develop this project.

By utilizing a test can for the fin layup, the ARS subgroup determined that the carbon fiber layup was strong and could withstand a harsh landing. Using Ansys Fluent and custom software, the FDA subgroup was able to accurately model the flight of the rocket. From a SolidWorks model, the PTSS subgroup found using COMSOL that the thermal loads on the motor mount would not negatively impact its structural integrity. Furthermore, the ANSYS simulations supported this finding for the linear application of the motor's maximum thrust value.

## Acknowledgements

The project team thanks the following individuals for their support and assistance throughout the project:

- Project advisor Professor Taillefer for his useful experience and continuous critique and acknowledgement of project work.
- Professor Hera for her ANSYS, Fluent and COMSOL software training to WPI's aerospace student body.
- Joanne Tripp for her assistance in the ordering process for project materials.

# Table of Contents

Abstract.....	2
Acknowledgements.....	3
Figures .....	6
Tables.....	8
1. Introduction.....	9
1.1 Executive Summary .....	9
1.2 Project Goals.....	10
1.3 Project Design Requirements, Constraints, and Other Considerations .....	11
1.3.1 Design Requirements .....	11
1.3.2 Design Considerations .....	12
1.3.3 Safety Considerations .....	12
2.0 Background and Literature Review .....	16
2.1 Model Rocketry Design Review .....	16
2.1.1 Airframe and Recovery Systems.....	16
2.1.2 Innovative Design Considerations .....	17
2.1.3 Airframe.....	21
2.1.4 Nose Cone.....	23
2.1.5 Recovery System.....	24
2.2 Flight Dynamics and Analysis .....	24
2.2.1 Overview.....	24
2.2.2 Flight Dynamics and Flight Performance Analysis .....	25
2.2.3 Flight Computer and Microcontroller .....	29
2.2.5 Structural Analysis.....	33
2.3 Propulsion, Thermal, and Separation Systems.....	34
2.3.1 Rocket Propulsion .....	34
2.3.2 Different Types of Rocket Engines and Propulsion Types .....	35
2.3.3 Model Rocket Propellants and Chemical Engines .....	36
2.3.4 Simulation and Testing of Rocket Motors .....	39
2.3.5 Mounting and Ignition .....	40
3.0 Methodology .....	44

3.1.1 ARS.....	44
3.2 Propulsion, Thermal, and Separation Systems.....	46
3.2.1 Thermal Analysis.....	46
3.2.2 NASA CEA Simulation.....	47
3.2.3 COMSOL Analysis: Problem Description and Assumptions.....	49
3.2.4 Heat Flux Physics and Governing Equations.....	50
3.2.5 Fluid Physics and Governing Equations.....	51
3.3 Flight Dynamics Analysis.....	53
4.0 Results.....	64
4.1 ARS.....	64
4.2 Propulsion, Thermal, and Separation Systems.....	64
4.2.1 NASA CEA Analysis.....	64
4.2.2 Physics Coupling and Results.....	66
4.2.2 Motor Structure Integrity.....	71
4.2.3 Innovative Design Theory.....	72
4.3 Flight Dynamics Analysis.....	74
5 Conclusions and Recommendations.....	79
5.1 Airframe Recovery System.....	79
5.2 Propulsion, Thermal and Separation System.....	80
5.3 Flight Dynamics Analysis.....	81
5.4 Broader Impacts.....	82
References.....	83

## Figures

Figure 1 Annotated Diagram of Rocket.....	16
Figure 2 Innovative Design Inspiration 3D Model .....	19
Figure 3 Innovative Design Idea Mechanism Housing.....	20
Figure 4 Innovative Design Idea Lift Arm.....	20
Figure 5 Early OpenRocket Design .....	22
Figure 6 SolidWorks Model.....	23
Figure 7 OpenRocket Model of HPMR .....	25
Figure 8 Predicted OpenRocket Flight of HPMR Rocket.....	26
Figure 9 RASAero Model of HPMR .....	27
Figure 10 RASAero Model Rocket Trajectory .....	28
Figure 11 RASAero Drag Coefficient versus Mach Number for HPMR .....	29
Figure 12 Wiring Diagram.....	30
Figure 13 Sled Model.....	31
Figure 14 Sled Model in Body Tube with Bulk Heads.....	31
Figure 15 Completed sled with sensors and batteries .....	32
Figure 16 FinSim Model of Trapezoidal Design .....	34
Figure 17 Liquid Propellant Rocket Diagram (NASA, 2021) .....	38
Figure 18 Model Solid Rocket Engine (NASA, 2021) .....	39
Figure 19 Motor Mount Diagram.....	40
Figure 20 Motor Mount Inside the Airframe .....	41
Figure 21 Engine Block Configuration.....	43
Figure 22 Example Electrical Ignition Schematic .....	43
Figure 23 Combined OpenRocket Design .....	44
Figure 24 Combined SolidWorks Design .....	44
Figure 25 Picture of Completed Fin Jin from 2022-2023 MQP .....	45
Figure 26 New Fin Jig in Use with New Fins.....	46
Figure 27 Heat Flux Boundaries .....	50
Figure 28 Fluid Boundary in COMSOL .....	52
Figure 29 CFD Geometry and Boundary Conditions .....	55
Figure 30 Supersonic Case Cross Section Mesh.....	56
Figure 31 Histogram of Number of Cells versus their Skewness .....	57
Figure 32 Y-Plus for Mach 1.05 .....	59
Figure 33 Mass Imbalance in the Solution for 210 m/s .....	60
Figure 34 Mach Number Contour for Mach 1.05, Angle of Attack of 0 degrees .....	61
Figure 35 Static Pressure Contour for Mach 1.05, Angle of Attack of 0 degrees.....	62
Figure 36 Mach Number Contour for Mach 1.05, Angle of Attack of 10 degrees .....	63
Figure 37 Static Pressure Contour for Mach 1.05, Angle of Attack of 10 degrees.....	63
Figure 38 Completed Rocket Assembly .....	64
Figure 39 Heat Transfer Distribution.....	67
Figure 40 2D Heat Transfer Distribution.....	68
Figure 41 Temperature Distribution Across Motor Assembly .....	69
Figure 42 Fluid Velocity in Motor.....	70
Figure 43 Deflection on Motor Mount, ANSYS Fluent simulation.....	71

Figure 44 Max Stress on Motor Mount, ANSYS Fluent simulation.....	72
Figure 45 Supersonic Solution, OpenRocket Simulation .....	72
Figure 46 Deflection on Motor Mount, Supersonic .....	73
Figure 47 Max Stress on Motor Mount, Supersonic .....	73
Figure 48 FinSim Theodorsen Calculations for Velocities .....	74
Figure 49 FinSim U-g Calculations for Velocities .....	75
Figure 50 CFD Drag Data.....	76
Figure 51 CFD Drag Model versus RASAero .....	77
Figure 52 Altitude and Velocity versus Time, 6DOF.....	78
Figure 53 Altitude and Velocity versus Time, OpenRocket .....	79

## Tables

Table 1 Cherry Limeade Propellant Composition .....	47
Table 2 CEA Output Values .....	48
Table 3 Analysis Results for Max Side Length and Drag Force.....	60
Table 4 Composition of Exhaust Gas .....	65



# 1. Introduction

## 1.1 Executive Summary

The project team was divided into three subgroups: Airframe and Recovery Systems (ARS), Propulsion, Thermal and Separation Systems (PTSS), and Flight Dynamics Analysis (FDA), according to their project goals and responsibilities, which are explained in detail in Section 1.2. A final set of responsibilities, Flight Operations, was assumed by the Airframe and Recovery Systems subgroup, since these concerned the selection, programming, and test of processors for control/monitoring of flight events or payloads.

The team designed, analyzed, and fabricated a single-stage, high-powered rocket. The team used the open-source software, OpenRocket, to create an initial design of the rocket. The ARS subgroup decided upon a fiberglass body, with an inner diameter of 66 mm or about 2.6 inches, and a wall thickness of 2 mm or about 0.08 in. The non-standard rocket body tube size allows fiberglass to be used to reduce weight without substantially increasing costs. The ARS subgroup selected fiberglass due to its structural strength, lower weight, and reliability among the hobbyist model rocket community. The team selected trapezoidal fins with a plywood core and tip-to-tip carbon fiber layup, and a commercial of the shelf (COTS) fiberglass nosecone to sustainably conserve costs and save time from making one.

The selected motor aimed to support the weight of the rocket with a fiberglass body with a simulated apogee of 1500 feet. The team has considered a black powder mode for separation of the body tube and nose cone to deploy the parachute. This was due to its reliability in the model **rocketry** field, lack of residue unlike black powder, and low cost.

## 1.2 Project Goals

The three overall project goals were as follows:

- Design, build, and fly a reusable rocket to an apogee of 1500 feet.
- Provide students with the opportunity to work as a team to design, build, and test a moderately complex aerospace system in which the overall vehicle performance is critically tied in with the mass and performance of the individual components and assemblies.
- Provide students with specialized training in and opportunity to apply software tools: MATLAB, ANSYS – Static Structural Analysis, ANSYS – Fluent, ANSYS – Dynamic Analysis, Cantera, and others

The ARS subgroup goals were:

- Airframe design, fabrication and assembly of overall mechanical structure and integration of other subsystems (SolidWorks, ANSYS)
- Design, fabrication, and test of innovative recovery system (SolidWorks, MATLAB)

The PTSS subgroup goals were:

- Selection, modeling, and test of (commercially available) motors for single and two-stage rockets as well as mounting and ignition system (SolidWorks, COMSOL, MATLAB, Cantera)
- Design, fabrication, and test of innovative stage separation systems (SolidWorks, MATLAB)
- Analysis of thermal loads from the motor(s) during flight (COMSOL, MATLAB)

The FDA subgroup goals were:

- Analysis of aerodynamic loads on the vehicle during flight (FLUENT, MATLAB)
- Selection, integration, and simulation of sensors for flight and vehicle dynamics, including accelerometers, gyros, and altimeter (MATLAB).
- Analysis of rocket performance (altitude, range, etc.) using commercially available software in support of design activities and flight planning. (MATLAB and specialized software TBD)
- Simulation of rocket flight dynamics (attitude angles and rates, acceleration) (MATLAB)

Additionally, the Flight Operations goals, which involved the entire project team, but especially the Airframe and Recovery Systems subgroup, included:

- Selection, programming, and test of processor for control/monitoring of flight events or payloads. (Arduino)
- Selection and testing of alternative approaches to tracking (through RF or optical beacons) the rocket during or after flight.

### 1.3 Project Design Requirements, Constraints, and Other Considerations

The baseline rocket design must comply with the design standards of the National Association of Rocketry for high-power model rockets (National Association of Rocketry, 2014)

#### 1.3.1 Design Requirements

- Use as much of last year's material as possible to conserve budget
- Utilize a black powder method for single stage separation
- Use a Level-1 impulse motor
- Use a camera in-flight

- Utilize flight computers to record and analyze the data

### 1.3.2 Design Considerations

- Rocket designed to obtain a ceiling altitude of 1500 feet
- The rocket designed to accommodate a carbon fiber body tube. This will reduce the weight and ensure structural integrity as opposed to solely fiberglass.

### 1.3.3 Safety Considerations

- Rocket simulations will occur before launch to ensure stability and safety
- The rocket must comply with the safety guidelines provided by the NAR (National Association of Rocketry, 2014)
- Only certified, commercially available model rocket motors are to be used
- The rocket must be launched with an electrical launch system and electric motor igniters
- The launch system must have a safety interlock in series with the launch switch
- Before launch, there must be a countdown and everyone must be at least 15 feet away when using D motors or smaller, and 30 feet when using larger rockets
- The rocket must be launched from a launch rod, tower, or rail that is pointed to within 30 degrees of the vertical
- If the rocket does not launch, the launcher's safety interlock must be removed, and a duration of 60 seconds must be counted before approaching the rocket.
- The launch location will be in an outdoor, open space. The project team is considering St. Albans, VT.
- The recovery system will include a parachute or streamer, so the rocket returns safely and undamaged to the ground.

- The project team must not attempt to recover the rocket from power lines, tall trees, or other dangerous places (Model rocket safety code - national association of rocketry, 2022).

## 1.4 Tasks

### ARS Subgroup:

#### Task 1:

- Problem Statement: Design and fabricate airframe structure (SolidWorks, OpenRocket).
- Solution: The subgroup designed and fabricated a fiberglass airframe with plywood fins and a carbon fiber overlay on the fins.
- Analysis Products: OpenRocket simulation to determine overall shape, size, stability and estimated weight, SolidWorks to model airframe and model subgroup components for weight allocation and spacing.

#### Task 2:

- Problem Statement: Lead integration of subsystems: payload, recovery, staging, avionics, and propulsion.
- Solution: Lead all subgroups in the integration of their components and the overall construction of the rocket.

#### Task 3:

- Problem Statement: Research both baseline and innovative recovery system.

- Solution: The baseline recovery system used at launch consists of a drogue and a main parachute. The innovative design considered and researched was a helicopter rotor blade recovery system, which ultimately was determined to not be possible.

#### PTSS Subgroup:

##### Task 1:

- Problem Statement: Selection, modeling, and test of (commercially available) motors for single and two-stage rockets as well as mounting and ignition system (SolidWorks, COMSOL, MATLAB, Cantera)
- Solution: The subgroup selected a motor based on the theoretical design of the rocket with a carbon fiber body. Should the project team opt for a fiberglass body, this motor will be re-analyzed and re-selected. The subgroup selected the Aerotech H283-ST motor.
- Analysis Products: OpenRocket simulation and SolidWorks model to estimate the total rocket mass.

##### Task 2:

- Problem Statement: Design, fabrication, and test of innovative stage separation systems
- Solution: The subgroup opted to analyze the structural deformation and theoretical integrity of the motor mount through the implementation of a supersonic motor.
- Analysis Products: ANSYS Fluent

##### Task 3:

- Problem Statement: Analysis of thermal loads from the motor(s) during flight

- Solution: Utilizing software for the calculation of chamber characteristics, including temperature, pressure, density, specific heats, and mean molecular weight, that will...
- Analysis Products: NASA CEA and COMSOL

FDA Subgroup:

Task 1:

- Problem Statement: Analysis of aerodynamic loads on vehicle during flight
- Solution:
- Analysis Products: Fin Sim Structural Analysis, 6DOF and ANSYS

Task 2:

- Problem Statement: Selection, simulation and integration of sensors for flight and vehicle dynamics
- Solution: Created sled using SolidWorks for sensor integration in rocket
- Analysis Products: SolidWorks

Task 3:

- Problem Statement: Analysis of Rocket performance and simulation of rocket flight dynamics
- Solution: Utilized commercially available software to accurately predict the rocket's flight trajectory. Additionally, created a 6 degrees of freedom model to add more accurate predictions using calculated data from ANSYS.
- Analysis Products: 6DOF, RASaero and Open Rocket

## 2.0 Background and Literature Review

### 2.1 Model Rocketry Design Review

The design of a successful model rocket follows the coalescence of aerodynamic, thermodynamic, and structural dynamic principles. The three subgroups of this project integrate these design considerations and test their effectiveness through software solutions. The principal components of a model rocket follow similar patterns as their full-scale alternatives: the nosecone, upper and lower airframes, main and/or drogue parachutes, and the motor tube.

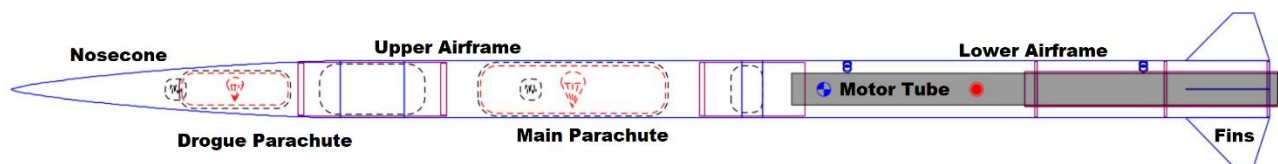


Figure 1 Annotated Diagram of Rocket

The body tube of the high-powered rocket possesses various payload elements such as a flight computer. High-powered model rockets follow the principles of rocket propulsion and implement H through O motors, classified by their total impulse values in  $lbf \cdot s$  ranging from 36.01-71.9  $lbf \cdot s$  for H, and up to 4604.01-9208  $lbf \cdot s$  for O (National Association of Rocketry, 2014).

#### 2.1.1 Airframe and Recovery Systems

One of the most important parts of any high-powered model rocket (HPMR) is the airframe, which serves as the structural foundation and aerodynamic shroud for the internal components. The airframe is a blend of form and function, requiring the precision of engineering and artistic design that makes model rocketry appealing to many enthusiasts. However, the



airframe is only one part of a HPMR's design. Equally integral to its success is the incorporation of a reliable recovery system to ensure the rocket does not plummet into the ground at high speed, endangering not only the rocket itself but also potential bystanders. The ARS team designs the airframe and recovery system. This team's scope is to design and construct the outer components of the rocket and select and implement the main and the drogue parachutes. The ARS team also assists with the integration of all components including the motor, payload, and parachute ejection.

The airframe holds all necessary components and therefore needs to be highly durable and resistant to changes due to factors like temperature. The airframe must remain rigid during the high aerodynamic loads around motor burnout to keep a consistent aerodynamic shape. The frame must be reliable and physically strong enough to survive a launch and reach the target apogee and all other specified flight parameters. To ensure success, materials for the body, nose cone, and fins must be selected carefully and purposefully to ensure reliability and that the flight parameters can be achieved.

### 2.1.2 Innovative Design Considerations

Most model rockets follow a similar design for the airframe and recovery systems, but when brainstorming innovative ideas for the recovery system, the team looked for ideas driven by concepts not executed on a large scale and only seen on smaller non-high powered model rockets. Unlike in previous years, the innovative design ideas the team investigated were not motivated by the ease of construction or convenience to fly. This project team investigated ideas that were interesting, coupled with the knowledge that the considered test sites do not allow non-standard recovery systems to be flown. The most interesting recovery system was a helicopter recovery system, where instead of a parachute, helicopter blades are deployed and spun around

to generate upward lift to slow down the rocket to safety. However, this recovery system only works well with small lightweight rockets. Furthermore, the flight location does not allow non-standard recovery systems.

The team also considered two other design ideas, umbrella recovery and parawing recovery. Umbrella recovery works similarly to a standard parachute. The point is to induce drag during the descent and decelerate the rocket. The team deemed it too similar to the standard recovery system and decided not to pursue the idea. The team also noted that the way the umbrella recovery system chutes attach and deploy are ideal for very lightweight small model rocket made from materials like cardboard. Being able to have the chute deployed in its intended manner would be a large challenge and unreliable.

The parawing recovery system is like a glider. Also called a Rogallo wing, the parawing is a modified circular parachute. The parawing is theoretically four to five times more efficient than a traditional ballistic parachute. However, there are difficulties in obtaining the perfect shape as the team would need to trim a regular parachute into the desired glider shape. As this recovery system functions as a glider, the rocket could glide miles away from the launch site and potentially land too far away to recover. The team did not want to pursue this design given its potential challenge, despite its proven success on a larger scale, having been used on the Gemini spacecraft.

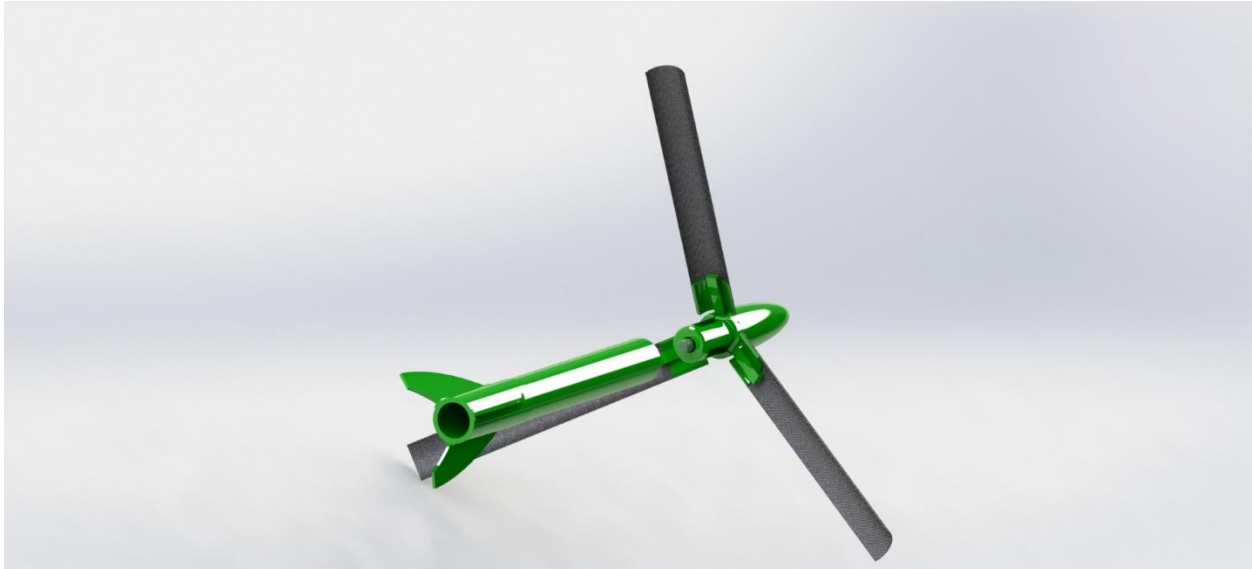


*Figure 2 Innovative Design Inspiration 3D Model*

The team found an initial design reference/inspiration, using a 3D printed model as the baseline for the design. The initial idea is a modified nose cone. The nose cone has a screw mechanism, where the piece that has the lift arms for the blades' screws in, making the nose cone and the lift arm holding piece attached. The design can be modified to have the piece simply attached using a coupler, similar to how two body tubes would be attached to the airframe of a rocket. Below is the reference idea before modification and full solidification.

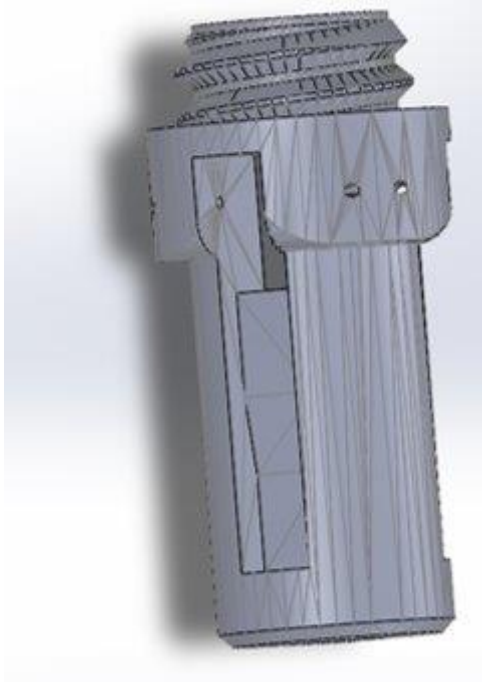


Figure 3 Innovative Design Idea Mechanism Housing

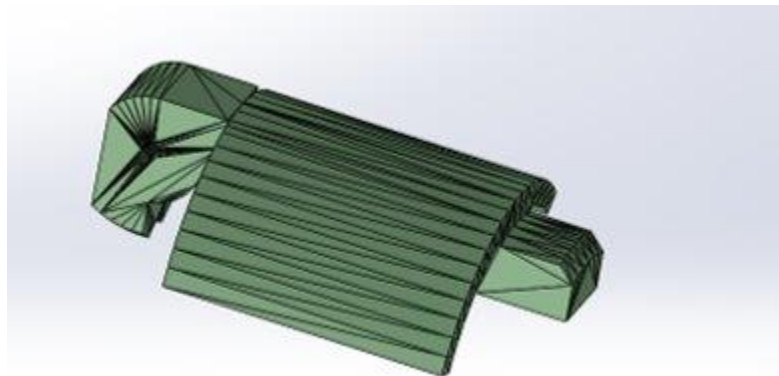


Figure 4 Innovative Design Idea Lift Arm

When analyzing the recovery system's feasibility, the team utilized the following equations to determine the required tip speed and rotations per minute (RPM) of the blades to achieve the required lift.

$$\text{Lift} = \text{weight } W = 24.50539 \text{ N}, A_{\text{body}} = 0.21 \text{ m}^2, A_{\text{blade}} = 0.70 \text{ m}^2, D = 6.8 \text{ cm},$$

$$L = \rho AV^2 \quad (1)$$

$$\text{Tip Speed (TS)} = \pi D \left( \frac{\text{RPM}}{60} \right) \quad (2)$$

Based on the calculations for the specified diameter and surface area, this recovery system was determined to be not possible. The required tip speed to allow lift to be equal to the weight of the rocket, was calculated to be about 18 m/s, making the required RPM over 5000 rpm. This is completely not possible, especially not using only a torsional spring to kickstart rotation. Normal helicopters blade RPMs lie between 200 and 500 RPM making this number of 5000+RPM completely unrealistic. Even in extreme cases such as the Mars Ingenuity helicopter, the blades only rotated up to 2500 RPM. To make this recovery system realistic, the proportions of the rocket must be drastically different, as it would need to be much wider in diameter and extremely light as well. Additionally, there would need to be a motor within the body that runs the helicopter blades for them to spin up even close to a speed at which they can adequately slow the rocket's descent.

### 2.1.3 Airframe

The design process of the airframe started simply. First the ARS team defined a goal as a constraint, which in this case was the goal altitude of 1500 feet. The team designed the initial airframe using fiberglass and plywood, considering these are popular materials for similar HPMR projects. The team decided that the body tubes of the airframe should be made of carbon fiber. Carbon fiber is similar to fiber glass, although fifteen percent lighter and significantly stronger. This would allow the use of a thinner body tube, saving even more weight. Carbon fiber is also less prone to expansion and contraction in extreme temperatures than fiberglass. The team additionally considered using a camera as a payload to see a rocket POV video of the flight. A window has been cut into the coupler where the camera will be held in order for the camera to record the flight.

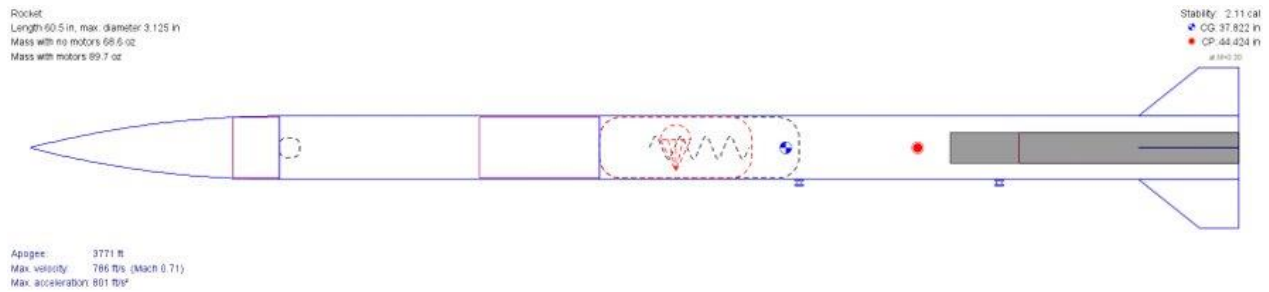


Figure 5 Early OpenRocket Design

After selecting the materials, the team used OpenRocket to create an initial design for the rocket including nose cone shape and fin shape, and how many fins. The below figure is an early design for the rocket in OpenRocket.

During the preliminary design processes, the team initially pursued elliptical fins due to their ideal shape for subsonic flight. This shape is ideal in theory as it displaces a smaller amount of air at the tips of the fins creating less drag. This is different in practice as the curved shape is difficult to properly manufacture, leading to a simpler shape with few straight edges is preferred. The final decision encompassed trapezoidal fins because the model rocket is considered a mid-size model rocket which will fly below the speed of sound, meaning the necessity to reduce drag as much as possible is not as great and therefore a smaller consideration. The team also intends to use a custom fin assembly rig like the jig created by the previous HMPR MQP, which supports a four finned rocket. The only difference in design between the fin jigs are their dimensions for the different sized rockets. Trapezoidal fins are also easier to manufacture compared to elliptical fins. Having sharp corners and flat edges is much easier than an elliptical contour to overlay using a fiber mesh and epoxy. The dimensions of the fins were determined by adjusting them slightly and checking the stability number in OpenRocket, aiming for a stability value of around 2-3 caliber, which is the distance between the center of mass and center of pressure measured in body diameters.



*Figure 6 SolidWorks Model*

A SolidWorks model was developed from the OpenRocket model. The team found a carbon fiber tube for the airframe, dictating the inner and outer diameter of the rocket. Based on the diameter values, a nose cone was found with the same inner and outer diameter.

Unfortunately, the originally selected tube was out of stock for purchase, but a similarly dimensioned tube made of fiberglass was found from a different retailer with the same inner diameters allowing the design to remain the same. The airframe has increased in length from the original iteration, as additional length was needed for the motor. The original length made fitting all components with additional room very tight the team wanted to incorporate more tolerance, as a contingency plan in terms of space.

#### 2.1.4 Nose Cone

There are many shapes of nose cones commonly used for model rockets. An ogive shape is preferred due to a smoother transition between the body tubes. Ogive nose cones have a lower drag coefficient than conic nose cones as the angle change is much more gradual than with a conic-shaped nose cone.

The specific nose cone the team decided on is a filament wound, fiberglass nose cone with a 4:1 ogive shape and a metal tip. Metal tipped fiberglass nose cones are quite common for a few distinct reasons. First, filament wound cones are a bit difficult to manufacture as it is hard to get the filament wound all the way to the tip. An aluminum tip also provides added stability and structural integrity. It can also take the brunt of the heat that the nose cone must hold up to, it

also can allow for higher impulse motors to be used in the case it is being used to fly higher and/or faster. An aluminum tip also allows for an eye bolt to be put at the very top of the nosecone, saving additional space for parachute and shock chord.

### 2.1.5 Recovery System

After the initial design of the rocket was completed in OpenRocket, the team used this simulation's weight estimate to determine a parachute size. A maximum safe ground hit velocity is 36 ft/s as given by the Spaceport America Cup Design, Test, and Evaluation Guide (Spaceport America Cup, 2023). Using an online calculator for parachute size by inputting those two values, the rocket's parachute should be between 42 and 56 inches if using a single parachute (RocketReviews, 2023). However, using a single parachute might make the rocket drift farther than desired, so the rocket uses a smaller drogue parachute as well as a larger main parachute to minimize the drift during recovery. When landing, potential damage could be as small as paint chipping or scratches but can be as severe as delamination of the layers of carbon fiber or fiberglass or in the worst case broken off fins or cracked airframes. That damage may compromise the structure and functionality of the rocket, so it is integral that the recovery goes as planned so that the rocket may be reused.

## 2.2 Flight Dynamics and Analysis

### 2.2.1 Overview

The Flight Dynamics and Analysis (FDA) team's responsibilities are to model and analyze the rocket's flight dynamics and performance parameters. Preliminary findings, using OpenRocket, RASaero and fin Sim, were used to determine the flight trajectory and parameters such as stability, drag coefficient, and center of pressure. ANSYS Fluent was used to compute various aerodynamic properties to model and visualize the forces acting on the rocket during



flight. These aerodynamic forces were used in custom flight dynamics software that will provide more accurate simulations of the flight. The FDA team's biggest contribution to the rocket is managing the flight computers, the TeleMega Flight Computer and RRC3 Altimeter System, which records telemetry data, detects apogee, and controls the deployment of the recovery system.

### 2.2.2 Flight Dynamics and Flight Performance Analysis

The first approach to analyzing the flight performance and dynamics of the model rocket was through the OpenRocket software. The design has a maximum diameter of 2.677 inches and a body tube length of 69 inches. The primary material is fiber glass, which was added to the OpenRocket simulation to allow for the most accurate analysis. In the below figure, the model rocket was created with our designated dimensions and recovery system.

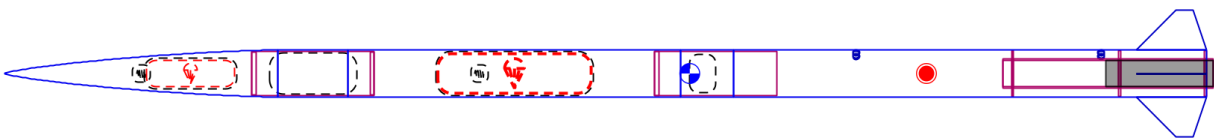


*Figure 7 OpenRocket Model of HPMR*

By using OpenRocket, the team initially simulated and predicted the apogee to be approximately 1456 ft. The goal apogee is 1500 ft based on previous launch site locations and regulations, so the rocket's design or motor must be modified. Our stability margin was also found to be 5.06, which is perfectly reasonable. A rocket with a stability margin below 2.0 is considered under stable and could become unstable if hit by strong enough gusts. A stability

margin above 3.0 is considered over stable which could result in weathercocking, which is when the rocket drifts into the wind. Generally being over stable is acceptable especially on larger rockets in the high-powered category, because the rocket is moving fast enough off the rail for the slight changes in wind only slightly affect the apogee and drift. So, our stability should be perfectly reasonable for our rocket.

OpenRocket is also able to provide a projected flight duration and path. It can also show when the recovery deployment period and the motor ignition and burnout.

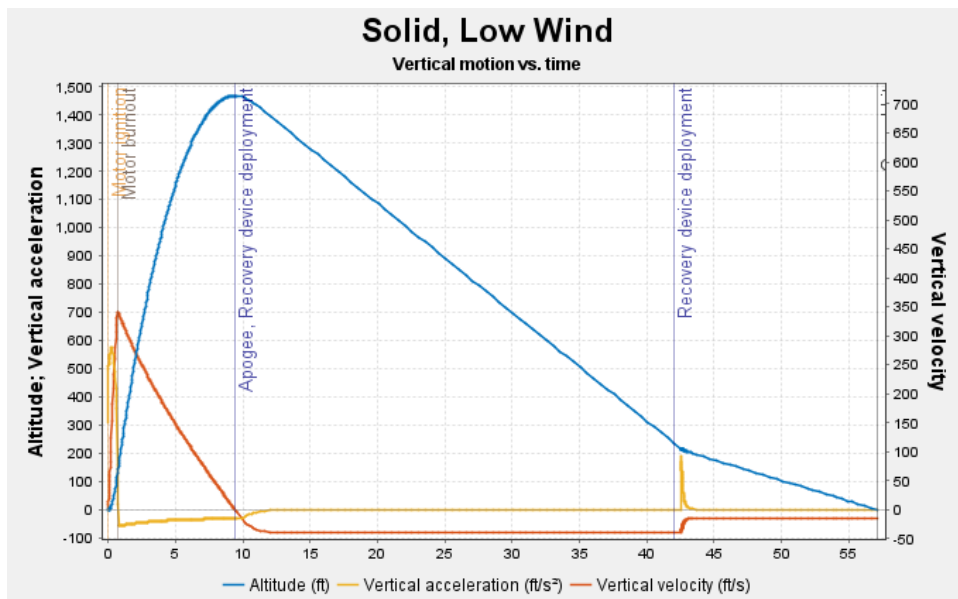


Figure 8 Predicted OpenRocket Flight of HPMR Rocket

One can see that the rocket reaches its peak altitude at around 10 seconds, at which point the drogue parachute deploys. Once the drogue deploys, the rocket can coast until it is time to deploy the main parachute for recovery and prevent more drifting. The second parachute is deployed at the 42 seconds mark, and finally impacts the ground at 14 ft/s at approximately 60

seconds. The motor ignition and motor burnout are relatively quick and occurs within the first 2 seconds of launch.

While OpenRocket is generally considered to be reliable software, the team also ran simulations using RASAero, which would provide more simulations to compare. In RASAero, the team created a model of the rocket with the same dimensions used in an OpenRocket, but with additional launch site details such as altitude, temperature, pressure, and wind speeds. With accurate launch conditions, RASAero should yield very accurate predictions, for its approximations of the rocket's fluid dynamics, of the rocket's position, trajectory, and velocity. The below figure shows the RASAero model, appearing almost structurally identical to the OpenRocket model. A 54-inch diameter parachute and 24-inch diameter rouge parachute were added.

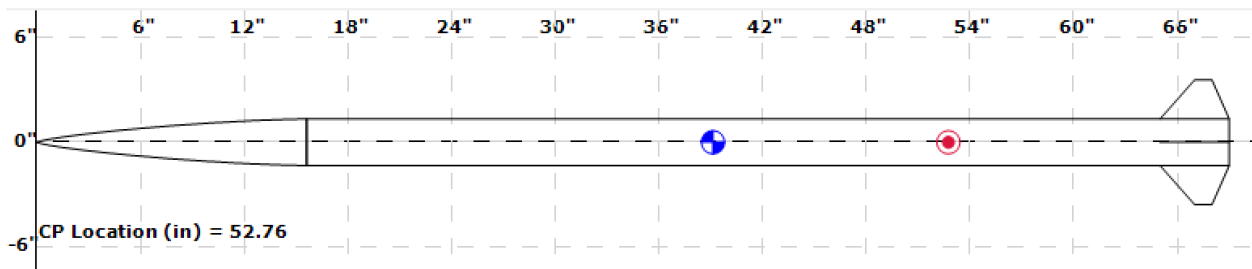


Figure 9 RASAero Model of HPMR

From the model, an H277 motor was used to simulate the results, as it contains almost identical strength to our motor, the H283. In doing so the team illustrates the differences between RASAero and OpenRocket. By running the simulation, the team approximated the apogee to be 1536 feet at a time of nearly 10 seconds. Figure 9 displays the rocket's trajectory with an impact time of about 55 seconds. At apogee, the drogue parachute is deployed, and the rocket slowly

glides to the ground. Then at an altitude of 500 ft, the main parachute is deployed and the rocket coasts to the ground, following the same flight path as OpenRocket.

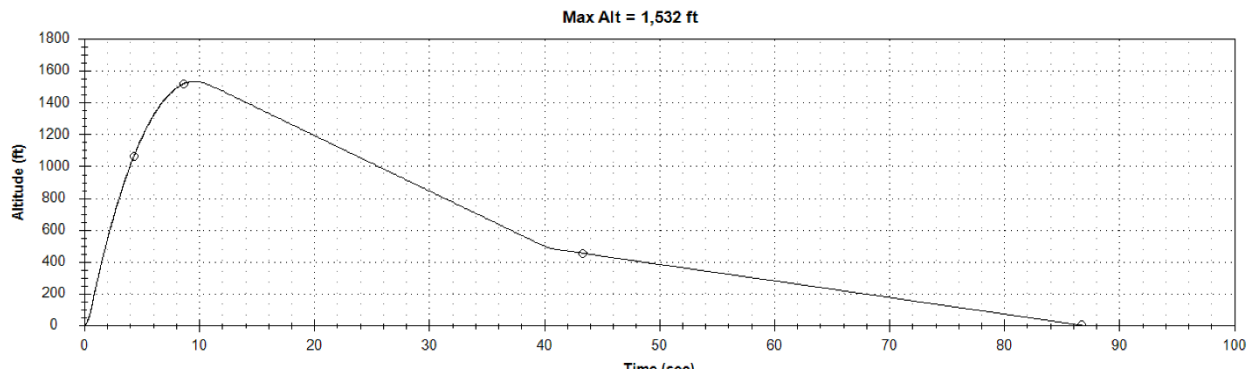


Figure 10 RASAero Model Rocket Trajectory

RASAero predicted flight is very similar to OpenRockets. Both models demonstrate that apogee will be reached in 10 seconds, and the rocket will land after about 60 seconds. RASAero does predict a slightly larger apogee, 1532 feet compared to 1456 ft, which is due to the RASAero model concentrating the total mass of the system in the motor. With a better distribution of the mass, the apogee would be closer to the 1500-foot limit. The RASAero model also deploys the main and drogue parachutes correctly and allows minimal drifting.

The OpenRocket model is more reliable as it can precisely add mass values throughout the rocket, allowing for a more accurate prediction. RASAero has created redundancy and assurance that the rocket will reach the proper altitude and follow a safe flight path.

Along with the trajectory, RASAero predicts the drag coefficient and the coefficient of pressure location which are found to be 0.383 and 52.755 inches respectively at Mach 0.7. Both values are very close to the OpenRocket values. Using RASAero, the team plotted the drag coefficient against Mach number across a flight, which demonstrates the peak of drag and the slow decline as the rocket begins to move faster.

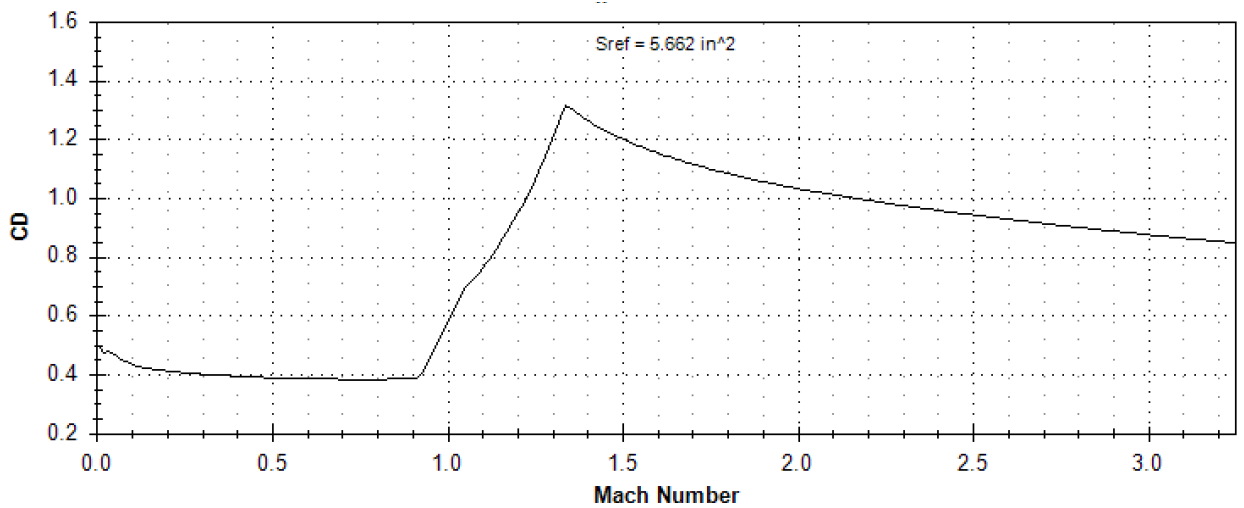


Figure 11 RASAero Drag Coefficient versus Mach Number for HPMR

Both RASAero and OpenRocket have provided the team with insight on the model rocket's predicted apogee, drag coefficient, center of pressure and time of impact.

### 2.2.3 Flight Computer and Microcontroller

For the flight computer, the FDA team decided to use the TeleMega sensor as it includes all the capabilities that are needed for this rocket. For this project, the main components of the TeleMega that will be utilized are apogee detection, deployment of recovery system, storage of recorded flight data, and GPS for rocket retrieval. Although the goal apogee is 1,500 ft, the sensor can detect apogee above and below our goal. Once the sensor detects apogee, a signal will be sent to ignite the black powders, deploying the recovery system. The recorded flight data is most important after a launch to analyze the data. To test the TeleMega sensor, the FDA team used black powder and igniters to ensure that it can properly detect the necessary parameters. The team also included the RRC3 sensor for redundancy. The wiring diagram for both sensors and the batteries are as follows:

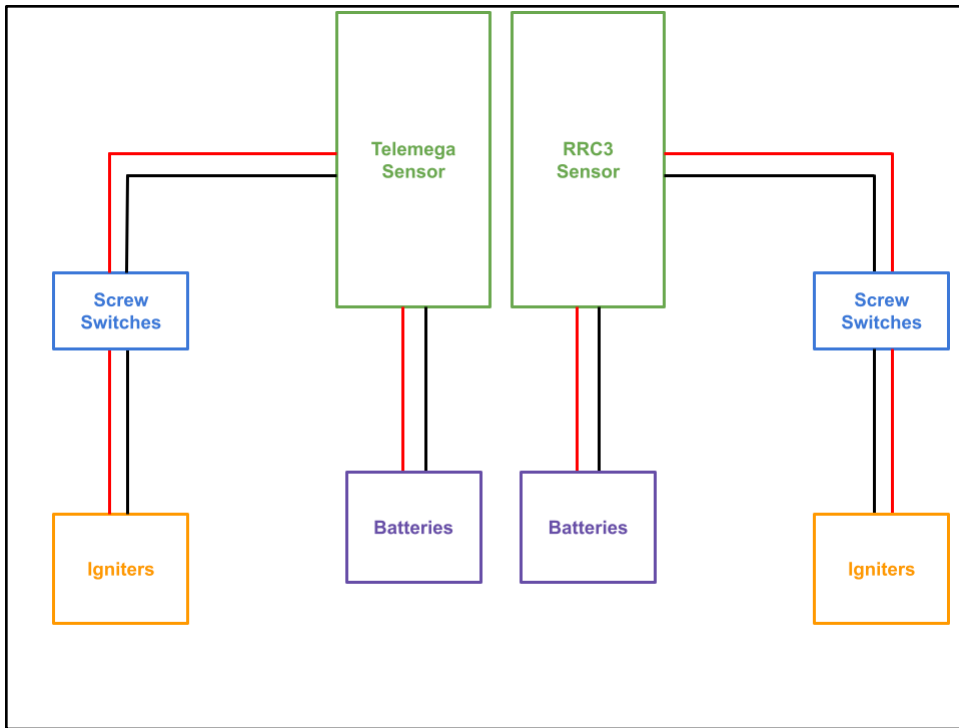
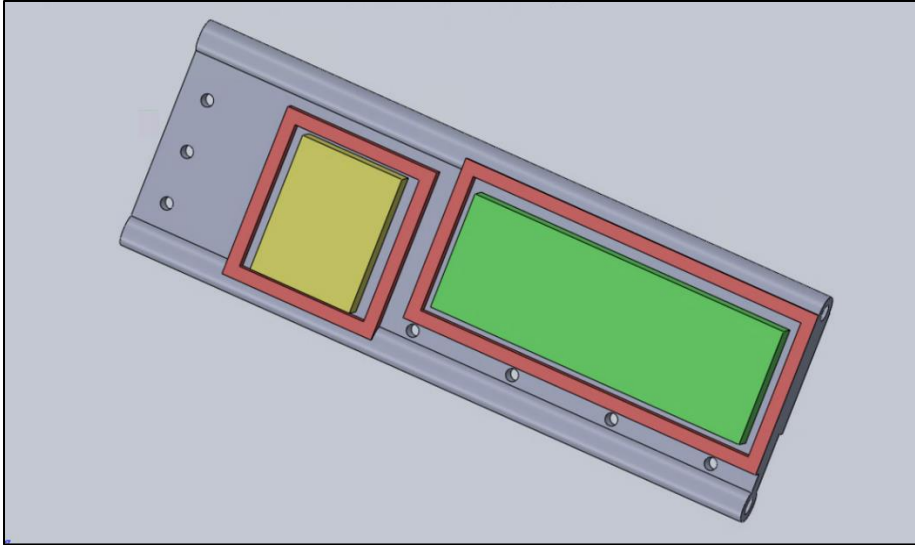
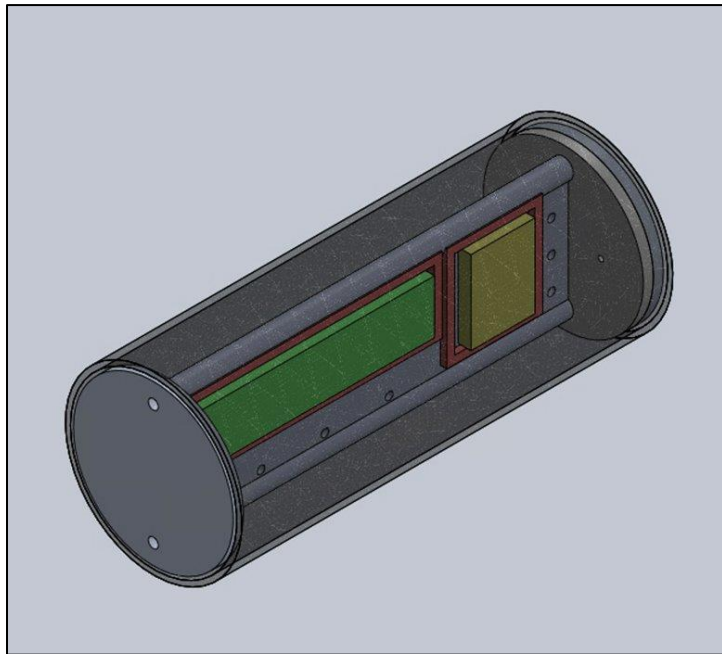


Figure 12 Wiring Diagram

The TeleMega, RRC3, and batteries will all be mounted onto a 3D printed sled. The sensors and batteries will be held into place with fasteners. For wiring purposes, there will be small holes throughout the sled. The SolidWorks model of the sled and the sled in the body tube are shown below.



*Figure 13 Sled Model*



*Figure 14 Sled Model in Body Tube with Bulk Heads*

In the SolidWorks models, the yellow blocks represent the batteries, the green blocks represent the sensors, and the red blocks represent where each component will be held into place. One side of the sled includes the dimensions for the TeleMega sensor (shown in Figure 13), and the other side has the dimensions for the RRC3 sensor (shown in Figure 14). The body tube was added into the model to show what the sled would look like in the tube, and the bulk heads were included to get an accurate reading of the sled mass, approximately 155 grams. Figure 15 shows the completed sled component.



*Figure 15 Completed sled with sensors and batteries*

Two 3.7V LiPo batteries were used to power the sensors. The FDA team determined it best to fully wire the sled before launch. The sensors and batteries were connected to show the completed sled but disconnected and removed afterward. During the testing phase, the FDA team



found that the 3.7V batteries worked the best for both sensors. In Figure 15, the bulk heads shown were 3D printed using PLA since there was difficulty with access to the machine shop. The sled was also 3D printed with PLA, and velcro straps will be used to secure the sensors and batteries in place before, which will be done before the launch.

### 2.2.5 Structural Analysis

FinSim is a structural analysis program used to determine the structural and aerodynamic properties of rocket fins. The program uses the Theodorsen and U-G methods of approximation to determine the fin's flutter and divergence velocities. Larger fin flutter and divergence velocities create excess drag, which could limit our maximum altitude.

The divergence velocity is the maximum velocity before divergence of the fin, which is when the moment of the air is greater than the structural stiffness of the fin, causing the fin to be twisted (Fin Sim). The flutter velocity is the maximum velocity the fin can handle before it begins to oscillate in an unstable motion.

To determine the flutter and divergence velocities, FinSim declares that each fin is mounted on torsion and bending springs and the aerodynamic center is located at the quarter chord point (AeroFinSim). The divergence and flutter velocities are then computed using the Theodorsen or U-G methods. Our design uses 4 trapezoidal fins made from 1/8<sup>th</sup> inch plywood. As seen in Figure 16, the fin design from OpenRocket matches that of FinSim.

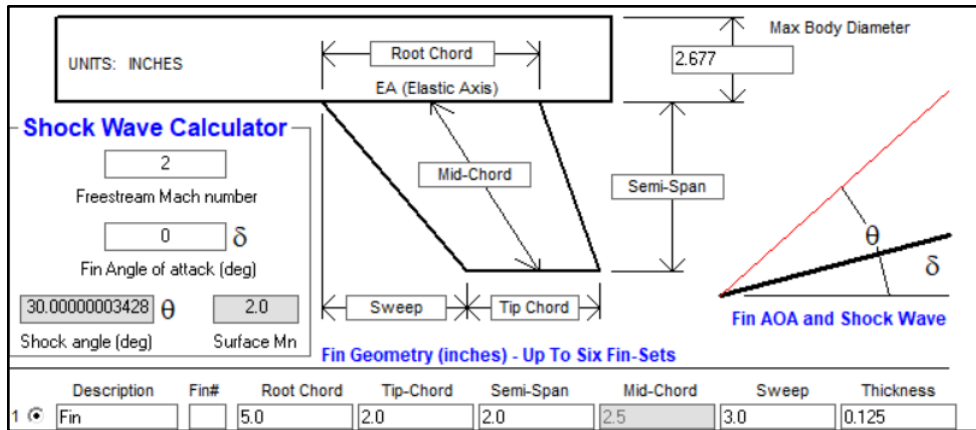


Figure 16 FinSim Model of Trapezoidal Design

## 2.3 Propulsion, Thermal, and Separation Systems

### 2.3.1 Rocket Propulsion

Rocket propulsion is derived from the concept of jet propulsion. Propulsion systems provide forces that move bodies initially, alter their current velocity, or overcome retarding forces when bodies are propelled through a viscous medium. Jet propulsion involves the imposition of a reaction force onto a vehicle by means of the ejected matter's momentum. Therefore, rocket propulsion can be defined as a form of jet propulsion in which thrust is produced by means of ejected matter, namely, the working fluid or propellant, which is stored within the vehicle.

The most common energy source in rocket propulsion is chemical combustion but energy can also be supplied using solar radiation or a nuclear reactor. The entire process begins when the ignition system activates combustion. Useful output thrust originates from the ejected matter's kinetic energy and the propellant pressure on the inner chamber walls and at the nozzle exit. In brief, rockets "work" by converting input energies, such as chemical sources, into kinetic

energy of the exhausted gas. It should be noted that the ejected matter may be of solid, liquid, or gaseous forms and at very high temperatures, of the plasma state. According to Newton's Second Law of Motion, the rocket is propelled in the direction opposite to the thrust or forced ejection of matter (Biblarz and Sutton, 2017, 1-5).

### 2.3.2 Different Types of Rocket Engines and Propulsion Types

The primary types of rocket engines are chemical, nuclear, and electric, with chemical being the most common. Chemical rocket engines usually fall into two categories: liquid propellant and solid fuel. There are additional gaseous propellant rocket engines and hybrid propellant rocket propulsion systems. Nuclear engines use a nuclear reactor, but due to public concerns over radioactive materials in Earth's environment, and their rarity overall, they will not be discussed in this report.

In chemical rocket engines, energy from the combustion reaction of chemical propellants (composed of a fuel and oxidizer), heats reaction product gases to high temperatures. These product gases are then expanded in a supersonic nozzle and accelerated to high velocities. Liquid propellant rocket engines, a form of chemical rocket engines, involve liquid propellants that are further fed under pressure from tanks into the thrust chamber. Bipropellants consist of a liquid oxidizer (such as liquid oxygen) and liquid fuel (such as kerosene). Monopropellants are composed of one liquid that decomposes into hot gases (such as hydrazine). Chemical propellants form hot gases inside the thrust chamber and are then accelerated through a supersonic nozzle. Finally, they are ejected at a high velocity, which, according to Newton's Second Law of Motion, yields a reaction force upon the vehicle (momentum). Supersonic nozzles are composed of a converging section, a throat, and a bell-shaped diverging section at the end.

The other common type of chemical rocket engine involves solid propellants. The burning components are already placed within a combustion chamber or case. The solid propellant (or charge) is termed the grain and contains all necessary chemical elements for complete burning. Once the grain is ignited, it should burn smoothly at a pre-established rate on all exposed internal grain surfaces. Unlike liquid propellant engines, there are no feed systems or valves involved in this engine's design.

Although not as frequently utilized as liquid or solid propellant engines, gaseous propellant rocket engines incorporate stored high-pressure gas such as nitrogen, helium, air, or some other working fluid. These gases require heavy tanks and are typically used for low-thrust maneuvers or attitude control systems. When the gas is heated with electrical energy or due to the combustion of monopropellants in a chamber, its performance is improved and is termed warm gas propellant rocket propulsion.

The final type of chemical engine incorporates both liquid and solid propellants, appropriately called a hybrid propellant rocket propulsion engine. For instance, the chemical reaction creates hot combustion gases when a liquid oxidizing agent is fed into a combustion chamber that is already filled with a solid carbonaceous fuel grain (Biblarz and Sutton, 2017, 5-12).

### 2.3.3 Model Rocket Propellants and Chemical Engines

Model rockets typically use either solid or liquid propellant chemical engines. In liquid model rockets, the fuel and oxidizer are stored separately and then pumped into the combustion chamber. In solid propellant model rockets, the fuel and oxidizer are combined into a single solid propellant which is inside a solid cylinder. Then, the propellant burns when exposed to a source of heat (unlike under normal atmospheric conditions). This ignitor is usually located at the end of

the propellant closest to where the nozzle begins. In this way, as the propellant begins to burn, the exhaust gases leave through the nozzle and generate thrust and a “flame front.” This process proceeds until the propellant is completely burned in the case of a solid propellant rocket engine. However, for a liquid propellant rocket engine, this process can stop by means of halting the flow of fuel or oxidizer (therefore, eliminating thrust). Liquid rockets are usually heavier and more complex due to the pumps and valves required for the fuel-oxidizer reaction to occur, while solid rockets are easier to handle and can rest for years prior to firing (*Model Rocket Engine*, NASA, 2021).

Usually, model rockets use solid propellants as composite or black powder varieties. Throughout history, black powder has been created from Potassium Nitrate, Sulfur, and Charcoal. This mixture would either be compressed mechanically or solidified through the addition of a rubber material such as Arabicum (natural rubber). This ensures that combustion is smooth and without fast burning unlike if the mixture remains in its powder form. The propellant has long been replaced by much more energetic, mechanically strong, and stable chemicals due to its low specific impulse, hygroscopic nature, and powdery form. Composite propellants might contain varying amounts of Ammonium Perchlorate, Strontium, and/or Barium Nitrate. These components are often in either solid or liquid form upon mixing. They are more powerful and are therefore used for larger engines (Yeshurun and Lulseged, 2020).

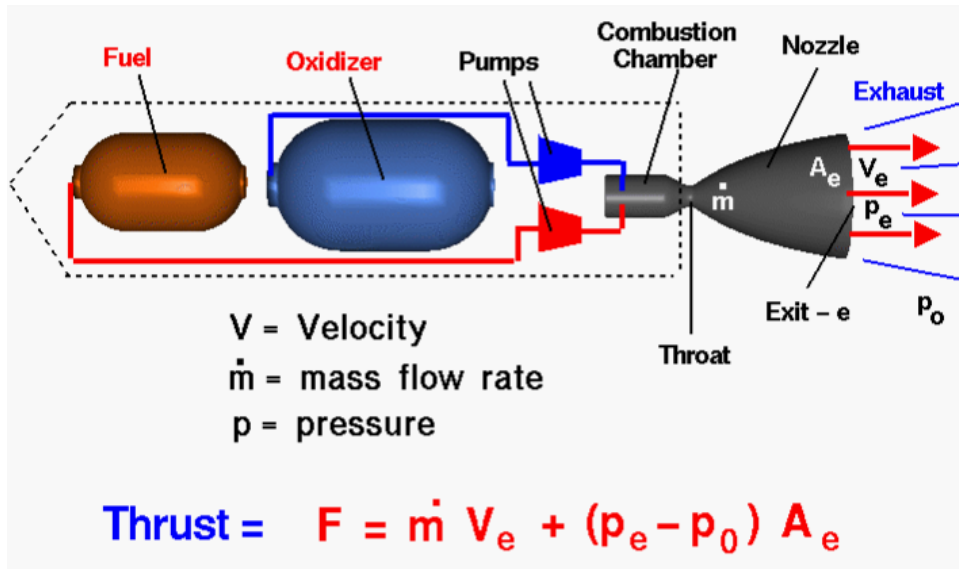


Figure 17 Liquid Propellant Rocket Diagram (NASA, 2021)

The diagram of a liquid propellant rocket. In order of ascending numerical value:

1. Liquid rocket fuel
2. Oxidizer
3. Pumps carrying fuel and oxidizer
4. Combustion chamber which mixes and burns the two liquids
5. Product gases which move through the nozzle throat
6. Exit exhaust (Liquid Rocket Engine, NASA, 2021)

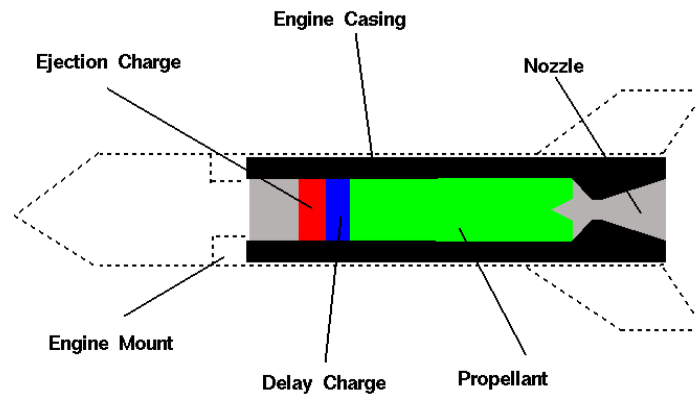


Figure 18 Model Solid Rocket Engine (NASA, 2021)

### 2.3.4 Simulation and Testing of Rocket Motors

There are a few applications that are particularly useful in simulating rocket motor performance. Firstly, OpenRocket can be used to simulate the flight of the rocket. However, to simulate the performance of individual motors, the open-source software, Open Motor, would be a more appropriate option. This allows the user to get various performance characteristics of a motor based on the input parameters such as nozzle and grain geometry.

MATLAB can be used for custom calculations to confirm the results of Open Motor. While development of a working MATLAB application is beyond the scope of this project, a similar environment to Open Motor could be achieved. Simulations of prospective motors are important, but test firing the physical motors is equally as important. Using a load cell fixed to a test stand, the team can get the physical data of the motor performance at our specific atmospheric conditions. This will allow the team to adjust simulated data if needed.

### 2.3.5 Mounting and Ignition

One of the most critical design components in the high-powered model rocket is the motor mount. This piece of hardware holds the motor securely in the centerline of the rocket, allowing unidirectional thrust. If the mount is not perfectly concentric or does not properly secure the motor, rocket performance will be compromised.

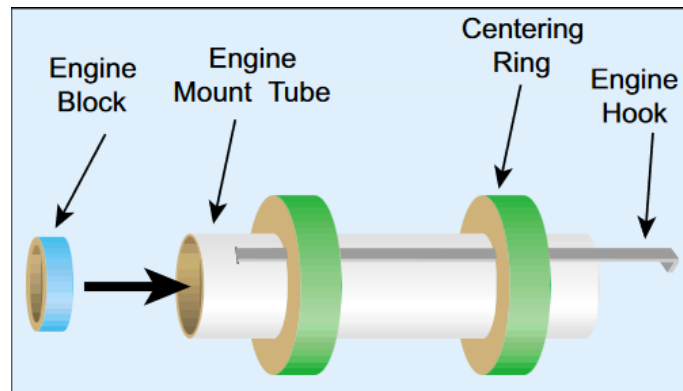


*Figure 19 Motor Mount Diagram*

For this project, the team will be using commercial off the shelf (COTS) motors, meaning that the motor will be shipped with the propellant and casing ready to launch. For this reason, thermal considerations of the mounting material do not have to be heavily considered when designing the mounting tube. The “engine mount tube” is typically made from high quality rolled paper and is available for purchase at a very affordable price. These mount tubes come in different sizes and materials based on the motor geometry, so it would be more cost efficient to purchase one rather than attempt to manufacture one for this project. The centering rings are typically made from materials such as paper, cardboard, or lightweight wood. They must be perfectly concentric with the mounting tube and must be secured to the tube with adhesive such as glue or epoxy (Apogee Rockets, 2021). For maximum performance and precision, the



centering rings will be laser cut from lightweight wood. These need to be custom manufactured to fit into the body of the rocket with a tight tolerance. The thickness of the mounting rings can be changed, so making them as thin as possible while preserving structural integrity will allow optimal performance of this hardware.

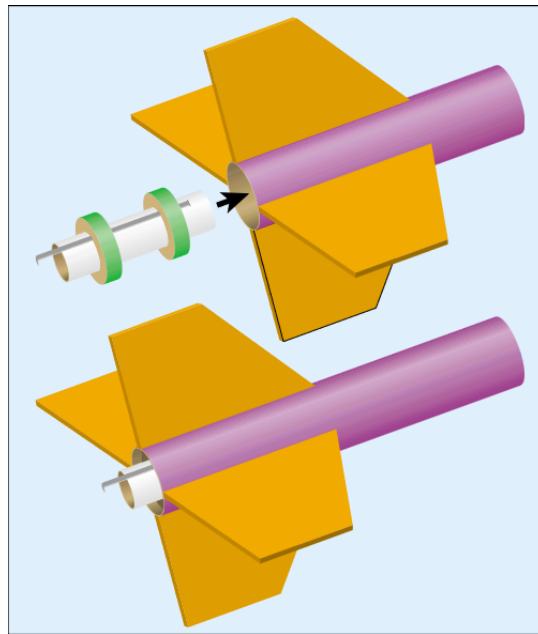


*Figure 20 Motor Mount Inside the Airframe*

The next component of the motor mount is the engine hook. Engine hooks are high-strength pieces of metal or plastic that securely hold the rocket motor in place. When using a parachute for recovery, there are often small explosive charges that separate the rocket airframe into small parts to descend in a controlled fashion. If the altimeter causes the charges to blow while the motor is still firing, the engine hooks will restrain the motor from flying out of the aft end of the rocket into the payload. COTS motors will typically have a notch at the aft end of the motor allowing for easy engine hook access. While an engine hook is not required to build a successful motor, they are extremely useful for quick reloading of the motors after firing.

A more general and inexpensive way to secure the motor is an engine block. The engine block is another motor retention technique that secures the motor from the outside of the body mounting tube. An engine block can be created by wrapping the exposed body mounting tube in a few turns of masking tape. With proper tolerances, the motor will stay in place for the flight with an extremely low-cost solution.

The most common ignition system in model rocketry is an electric ignition system. For the rocket motor to ignite, a small, high-resistance wire is inserted into the nozzle, contacting the propellant. When electricity is run through the wire, it heats up, causing the propellant to ignite and eject the wire out of the nozzle during takeoff. Electric ignition systems typically have a launch control box where the ignition sequence is carefully initiated to maximize safety and launch preparedness. An example of a rocket ignition system schematic can be seen in Figure 22. Most launch locations will have ignition systems readily available for groups to use, so designing one from scratch would not be necessary for this project.



Figure 21 Engine Block Configuration (Apogee Components, n.d.)

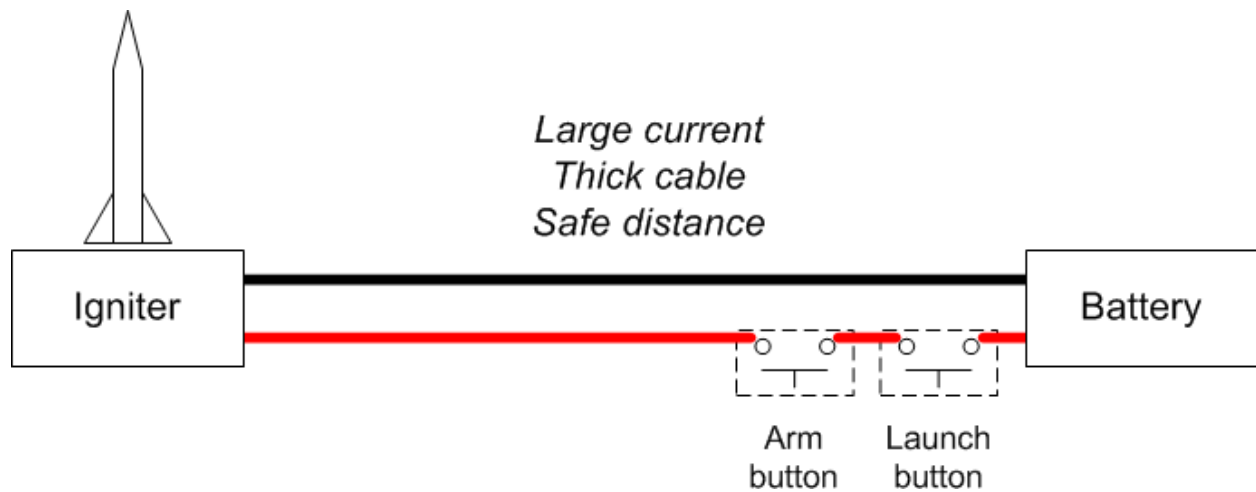


Figure 22 Example Electrical Ignition Schematic

### 3.0 Methodology

#### 3.1.1 ARS

The initial design was completed around a carbon fiber tube that the team found online, however that specific carbon fiber tube is out of stock, so a new tube and nose cone needed to be selected. A similar tube was selected as a replacement, with a 66mm inner diameter and 70 mm outer diameter and a fiberglass nosecone was found with the same dimension. This would allow the inner components to stay unchanged due to any changes in diameter. -As seen below, the combined motor design would work for the solid and hybrid motor and as this was a consideration, the rocket was made longer to accommodate. Later in the design process, the team considered the possibility of using a larger rocket motor to potentially fly a supersonic rocket. The design would have minimal changes, mainly to the fins, which can be seen by comparing Figures 23 and 24.

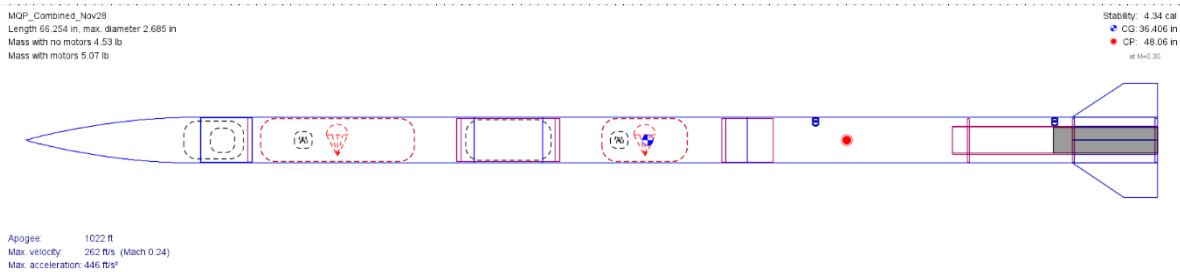


Figure 23 Combined OpenRocket Design

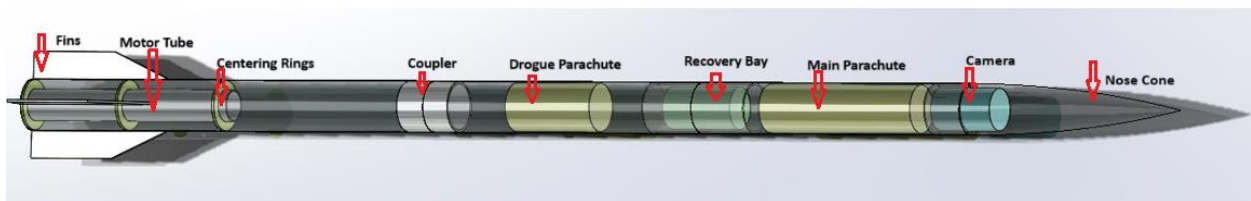
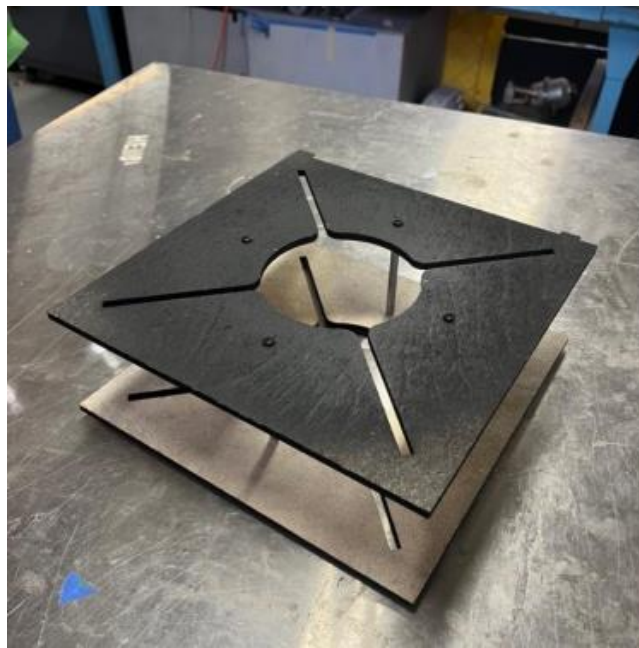


Figure 24 Combined SolidWorks Design

### 3.1.1 Fin Jig

To assemble the fins onto the rocket, they need to be epoxied onto the body and held in place until the epoxy cures. To ensure that the fins are cured in a correct alignment, a fin jig may be used. The design of the fin jig is similar to the fin jig designed by the previous year's MQP team. However, this team's fin jig is smaller to account for the smaller rocket diameter and fin size.



*Figure 25 Picture of Completed Fin Jin from 2022-2023 MQP*



*Figure 26 New Fin Jig in Use with New Fins*

## 3.2 Propulsion, Thermal, and Separation Systems

### 3.2.1 Thermal Analysis

There are a few software tools that can be employed to analyze the thermal loads from the motor during flight. First, NASA's CEA software is going to be used to estimate both the chamber temperature and the propellant exhaust composition. While CEA results give information about the thermochemical reactions involved in the flight, analysis in COMSOL allows the team to use those results and apply them to a geometry. COMSOL is a multiphysics platform that will aid the team in showing the thermal loads within the airframe and mounting system from the motor. Between COMSOL and CEA, the team will be able to successfully analyze the thermal loads from the rocket motor during flight.

### 3.2.2 NASA CEA Simulation

NASA's Chemical Equilibrium with Applications (CEA) software was used to estimate the chemistry of the rocket motor. It is important to note that COTS motors from manufacturers such as Aerotech and Cesaroni keep their proprietary propellant mixtures as a trade secret meaning the exact molarity of the reactions are not available for use in this analysis. Instead, the propellant composition will be modeled after MIT's Cherry Limeade recipe seen in Table 1 (Fallon, 2021).

*Table 1 Cherry Limeade Propellant Composition (Fallon, 2021)*

Ingredient	% of Total
HTPB	10.88%
IDP	4.28%
MDI	1.94%
Castor Oil	0.30%
PDMS	0.05%
Triton X100	0.05%
Aluminum Powder	7.5%
200 AP	65.5%
90 AP	9.5%

The CEA analysis started by selecting the problem type as a rocket with a pressure of 1000 psia. Defining the fuel and oxidizer required some simplification of the composition listed above. First, since there is no specific formula for hydroxyl-terminated polybutadiene (HTPB), the chemistry for this will be replaced with butadiene or C<sub>6</sub>H<sub>4</sub>. The fuel will be defined as 30%

aluminum powder and 70% butadiene, and the oxidizer is defined as 100% ammonium perchlorate or  $\text{NH}_4\text{ClO}_4$ . The reaction temperature was defined using the motor's datasheet at 515K, and the oxidizer to fuel ratio was set at 4. From there, the software was able to generate the following parameters of interest.

Table 2 CEA Output Values

Parameter (Chamber)	Value
Pressure, P	69 bar
Temperature, T	3201 K
Density, $\rho$	6.102 $\text{kg}/\text{m}^3$
Enthalpy, H	-886.24 kJ/kg
Molecular Weight, M	23.24 kg/kmol
Specific Heat Ratio, $\gamma$	1.169

The values shown in Table 2 allow the calculation of desired rocket parameters to be estimated. The results of CEA analysis included some desired performance parameters that will help estimate the thrust that the motor can produce using equation x.

$$T = \dot{m} I_{sp} g_0 \quad (3)$$

One of the performance parameters given by CEA is the specific impulse at a value of 166s. Knowing that  $g_0$  is the gravitational constant of Earth,  $\dot{m}$  can be found by dividing the propellant mass of 0.097 kg by the burn time of 0.7s to get 0.1386 kg/s. Plugging these values



into equation x, it is estimated that the motor produces an average thrust of around 226 N. This value is in the reasonable range for category H motors and can visually match the thrust curve supplied by the manufacturer.

### 3.2.3 COMSOL Analysis: Problem Description and Assumptions

During the combustion process, the solid propellant is chemically turned into a high-pressure, high temperature gas and expelled through the motor's nozzle. To accurately model the physics involved in the motor, both heat transfer and fluid flow must be solved simultaneously. The COMSOL Multiphysics software allows for the coupling of what would be separate physics problems to allow key heat flux parameters to be numerically calculated for a given motor.

The objective of the COMSOL analysis is to understand the thermal loads the motor and surrounding hardware will experience from the combustion process. According to the manufacturer, the propellant will ignite at 515K. From there, the propellant will burn and in doing so will cause a heat flux to the casing and mounting hardware. This analysis will allow the team to quantify this heat flux in the presence of fluid flow and choose appropriate materials accordingly.

The first assumption to be made is that the propellant grain pattern is perfectly circular. This will allow for the assume that the distribution of propellant, and thus the exhaust gas will be axisymmetric. It will also be assumed that the propellant burns steadily, allowing for a simple burn rate to be calculated by dividing the mass of the propellant by the burn time (both given from the manufacturer). An axisymmetric cross section can be modeled easily in COMSOL using these conditions.

### 3.2.4 Heat Flux Physics and Governing Equations

COMSOL will be used to first solve for the thermal flux produced by the motor during flight. During the 0.7 second burn time, the chemical reaction of the propellant will act as a convective heat source and increase the temperature of the surrounding material. With this heat source, there is a time dependence, as the components of the motor and mounting hardware can only experience a temperature increase during the burning of the propellant. A sketch of the model used can be seen in the figure below.

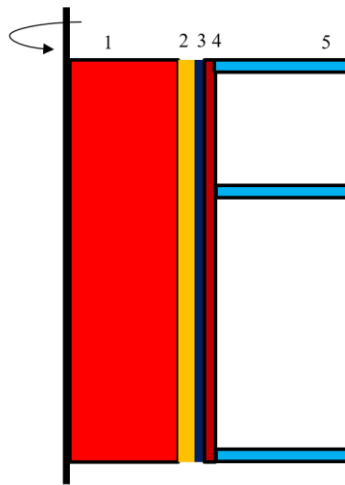


*Figure 27 Heat Flux Boundaries*

The first zone represents the combustion gas created upon igniting the propellant. The second zone is the propellant grain, the third zone is the aluminum motor casing, the fourth zone is the motor tube made from rolled paper, and the fifth zone represents the wooden centering rings. The bolded lines around the motor tube and centering rings represent the surfaces which are exposed to air at room temperature (298K). It is these materials that are crucial to analyze. Not only are they low temperature materials, but they are also responsible for keeping the motor

centered in the rocket, and any temperature related failures would result in total failure of the system.

COMSOL will solve the following equations for the time dependent advective heat flux through the layers of the motor.

$$\rho C_p \frac{\partial T}{\partial t} + \rho C_p \mathbf{u} \cdot \nabla T + \nabla \cdot \mathbf{q} = Q + Q_{ted} \quad (4)$$

$$\mathbf{q} = -k \nabla T \quad (5)$$

In this equation,  $\rho$  represents the density of the material through which heat flux will occur,  $C_p$  represents the constant pressure specific heat of the material,  $\mathbf{u}$  represents the velocity field,  $T$  represents the temperature,  $t$  represents the time,  $\mathbf{q}$  represents the heat flux by conduction,  $Q$  represents the heat flux from any additional sources and  $Q_{ted}$  represents the heat transfer thermoelastic damping. COMSOL uses numerical methods to solve this equation for the given cross section and gives data for the temperature distribution within the model. To accurately start this analysis, chamber values from the CEA analysis must be used. The chemical reaction occurs at the boundary between the propellant exhaust gas and the solid propellant grain. Therefore, setting a constant temperature heat source here (from CEA) can accurately represent the combustion process on the surface of the grain. With the geometry, materials, and initial conditions defined, one can get a value for the thermal loads experienced for a time dependent scenario.

### 3.2.5 Fluid Physics and Governing Equations

The fluid flow within the chamber must also be considered within the chamber. The fluid was modeled as a compressible, with the boundaries shown below.

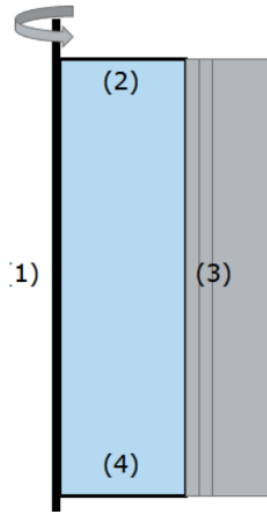


Figure 28 Fluid Boundary in COMSOL

The blue region represents the area where exhaust gas will flow. The first side of the region represents the line of axisymmetry within the chamber and is not a boundary which restricts fluid flow. The second side is modeled as a wall where fluid cannot flow. This represents the most forward section of the combustion chamber where the black powder charges would be located. The third side of the region is the boundary which the chemical reaction of the propellant occurs. It is in this region that the exhaust gas is produced, so it is modeled as a fluid source/inlet in COMSOL. This value was estimated using the data from the manufacturer as equation (1)

$$U_0 = \frac{\dot{m}}{\rho A_{grain}} \quad (6)$$

In this equation,  $\dot{m}$  represents the mass flow rate of the motor,  $\rho$  represents the density of the exhaust gas, and  $A$  represents the surface area of the propellant grain on the inside of the motor at the beginning of the burn. The fourth side represents the area immediately before the nozzle in the chamber, being modeled as a fluid outlet in COMSOL. This is simply defined using an outlet

pressure of 1000 psi. Using these initial conditions, COMSOL solves the Navier-Stokes equations seen below to find the behavior of the fluid.

$$\rho(\mathbf{u} \cdot \nabla)\mathbf{u} = \nabla \cdot [-p\mathbf{I} + \mathbf{K}] + \mathbf{F}$$

$$\nabla \cdot (\rho\mathbf{u}) = 0$$

$$\mathbf{K} = \mu(\nabla\mathbf{u} + (\nabla\mathbf{u})^T) - \frac{2}{3}\mu(\nabla \cdot \mathbf{u})\mathbf{I} \quad (7)$$

The first of the three equations in (2) represents the momentum equation where  $\rho$  represents the fluid density,  $u$  is the velocity field,  $pI$  is the pressure tensor,  $K$  is the stress tensor, and  $F$  is the sum of any external forces on the system. The second equation in (2) represents the conservation of mass in a fluid system, and the third equation defines the stress tensor,  $K$  in terms of velocity,  $u$  and dynamic fluid viscosity,  $\mu$ .

### 3.3 Flight Dynamics Analysis

The FDA team utilized the TeleMega sensor in the laboratory as our primary microcontroller. The TeleMega has an altimeter, accelerometer, GPS, and supports 4 pyro events. The creation of our own microprocessor was discussed, but ultimately unnecessary due to the TeleMega's extensive list of features. Additionally, the TeleMega was already purchased and required no additional expenses. Missiles Works RRC3 microcontroller is also integrated into the system as an additional data collection method. If the TeleMega were to break during flight, the RRC3 microcontroller would collect data allowing the team to still analysis the flight data. The added redundancy ensures that the flight trajectory will be collected.

### 3.3.1 Telemega Ignition Test

The purpose of testing our TeleMega sensor is to determine if it is functioning properly and capable of igniting a black powder charge. The sensor was connected to a 3.7 V LiPo battery and laptop. The sensor automatically powers on and displays previous flight log data. By clearing the previous flight log, the sensor was ready to simulate a launch. In a controlled and safe environment, a small black powder charge was attached to the sensor. The TeleMega is able to ignite the charge once instructed to by the users input command. Initially, the charge did not ignite due to connection issues with the power source and battery. Rewiring and connecting batteries to the sensor did solve this problem, and the sensor was able to complete a countdown and ignite several times. Brand new LiPo batteries are utilized for the launch date to ensure that no misfires occur.

### 3.3.2 Ansys CFD

To get an accurate model of the rocket's flight dynamics, the team first needed to know the aerodynamic properties of the rocket under the conditions that are expected to be experienced. Ansys Fluent was used to run a Reynold-Averaged Navier Stokes (RANS) computation fluid dynamics (CFD) simulation to find an averaged steady-state model of the flow around the rocket. The relevant aerodynamic forces collected are the forces and center of pressure in x, y, and z directions. The initial simulations with RASAero are used to get an idea about the flight conditions the rocket will experience.

The 3 input parameters vary in the CFD were velocity, angle of attack, and roll. The RASAero sim dictates that the max speed is going to be at Mach 1.05, so to allow for some

margin of error, a max velocity of Mach 1.2 was used. Using the 8 symmetry planes our rocket has, the team can cut down the range of roll angles from  $0^{\circ}$ - $360^{\circ}$  down to  $0^{\circ}$ - $45^{\circ}$ . As the rocket gets up to speed the range angle of attacks that the rocket may experience quickly falls to  $0^{\circ}$ , so for speeds below Mach 0.7, a range of  $0^{\circ}$ - $2^{\circ}$  was used, and for speeds above Mach 0.7, a range of  $0^{\circ}$ - $0.25^{\circ}$  was used.

The boundary conditions for the CFD are: a hemispherical velocity inlet with a radius of 2 rocket lengths, 1 rocket length away from the nose cone; a pressure far field going with a velocity matching the velocity inlet and 0 supersonic gauge pressure that starts tangent to the velocity inlet and goes down 6 rocket lengths below the bottom of the rocket; a pressure outlet with 0 gauge pressure as a circle constrained by the pressure far field; a rigid wall for the rocket geometry modeled with a equivalent sand grain roughness of 5 microns. An image showing the boundary conditions can be seen in Figure 29.

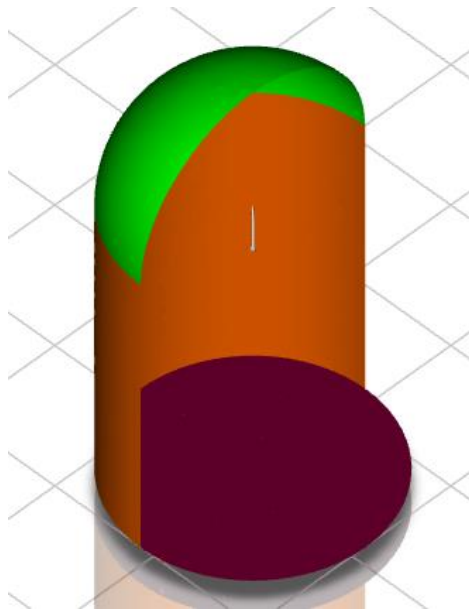


*Figure 29 CFD Geometry and Boundary Conditions*

To get accurate CFD results, a good mesh needs to be created. The mesh used was a poly-hexcore mesh created by Ansys's Fluent Meshing module. Fluent Meshing was used as it is able to take advantage of Fluent's ability, as a Finite Volume Solver, to both meshes made up of arbitrary polyhedrons and non-conformal meshes, where faces on a cell can match with faces from more than 1 other cell. A poly-hexcore mesh using a mesh that uses a structured grid of hex cells (cubes) refined into smaller hexes to match up to the polyhedral cells that bridge the gap between the boundary conditions and the structured grid. A cross section of the mesh used in the supersonic case can be seen in Figure 30. Edge lines were removed for visibility around the polyhedral cells.

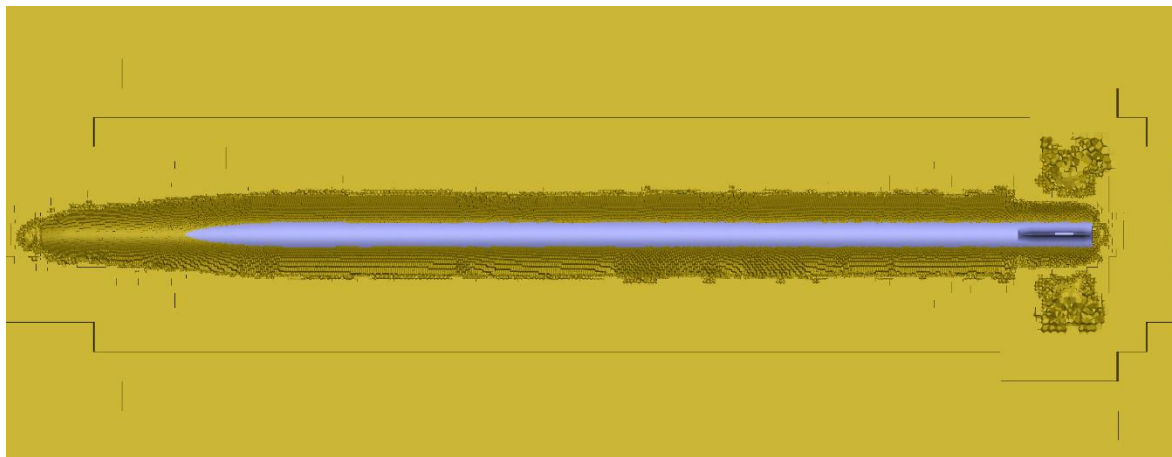


*Figure 30 Supersonic Case Cross Section Mesh*

A few things can be done to verify the ability of a mesh to capture all flow behavior. First and simplest is to check one of the many built in mesh quality metrics in Fluent Meshing, the one most relevant to the project is the cell's skewness. The skewness of a cell is the difference between the shape of a cell and of a cell of the same volume with equal side lengths. Skewness is measured on a scale of 0-1 with 0 being perfect and near 1 being highly skewed. As the hex cells



are already guaranteed to be an equilateral shape, they all have a skewness of 0. For the polyhedral cells, a skewness value above 0.95 can cause convergence issues. The mesh had a highest skewness of 0.80 and an average skewness of 0.04, which is within the desired range. A bar chart showing number of cells vs their quality can be seen in Figure 31.

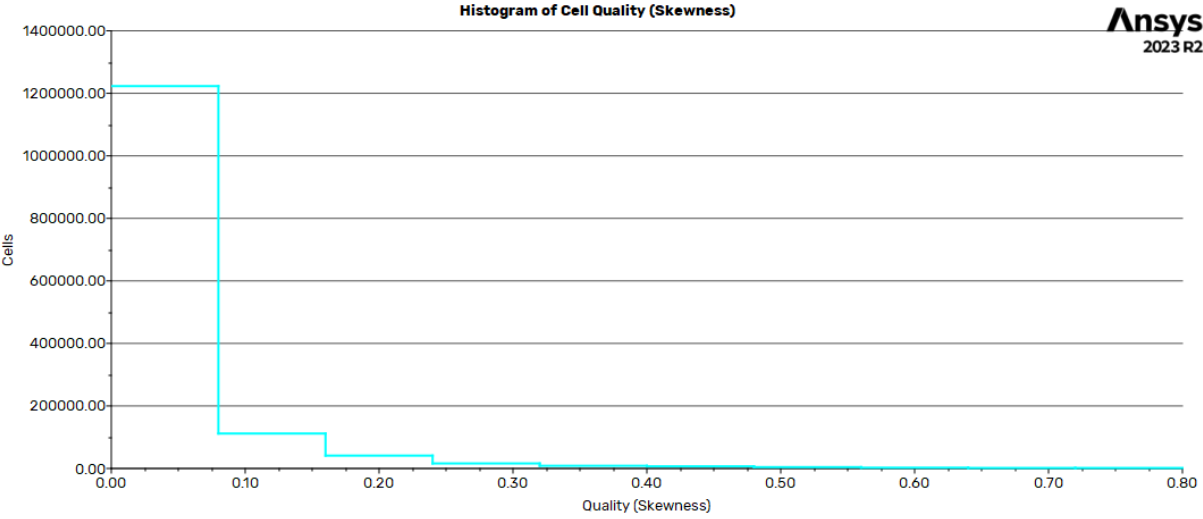


Figure 31 Histogram of Number of Cells versus their Skewness

For a mesh to properly wall the near wall behavior of the boundary layer, an appropriate y-plus value must be used for the wall function employed. Y-plus is a nondimensional number that relates how developed a boundary layer is to the distance from the wall, used along with u-plus, a nondimensional number relating how developed a boundary layer is to the velocity of the flow. The y-plus values targetted are in either the range 1-10 or 30-300 depending upon which wall functions are being used. The boundary layer can be separated into a few regions: the first of which has a range of 1-10 and is characterized by a linear increase in u-plus with increasing y-

plus; then there is the range 30-300 which is characterized by a logarithmic relation between  $y^+$  and  $y^+$ ; in between these 2 regions is a transition region that is not well characterized and is best to be avoided. (Ansys Fluent Theory Guide)

To target the desired  $y^+$  value, the team used inflation layers which allow the team to choose the height of the cells along the wall to reach our target  $y^+$  then grows to the size of the polyhedral cells near the rocket. The first layer height can be estimated while doing initial meshing, but the actual values need to be checked and first layer height can be adjusted until the targeted  $y^+$  range is reached.

For the subsonic cases, both wall functions were used as the slowest velocity (10 m/s) is an order of magnitude lower than the fastest velocity (210 m/s). The first layer height of 0.00036 m was chosen to put the  $y^+$  for the 10 m/s case on the low and the 30 m/s case on the high end of the linear  $y^+$  region, and the 210 m/s case was in the middle of the log  $y^+$  region so that the boundary layer is valid for all cases without requiring remeshing. The transonic and supersonic cases used only the log region of  $y^+$  as the first layer height decreases with increasing velocity for a constant  $y^+$  and using a higher first layer height allows the use of less cells for faster computation. The transonic case used a first layer height of 0.00022 m and the supersonic case used 0.00016 m.

The  $y^+$  for Mach 1.05 can be seen below in Figure 31. The estimated  $y^+$  value for this mesh was 100 which most of the cell are near. There's a slight increase in  $y^+$  where the flow is accelerated both on the tip of the tip of the nose cone and along the fins but is well within a safe range as  $y^+$  is only estimated to increase by about 20 in the fastest case. There are also small regions of  $y^+$  in the 10-30 range where the leading edge of the fins meet the body tube and on the bottom of the rocket, but these regions are both small and have slow moving flow, so

the boundary layer in those regions has minimal effect of the aerodynamic forces. Similar trends were found in both the transonic and subsonic cases.

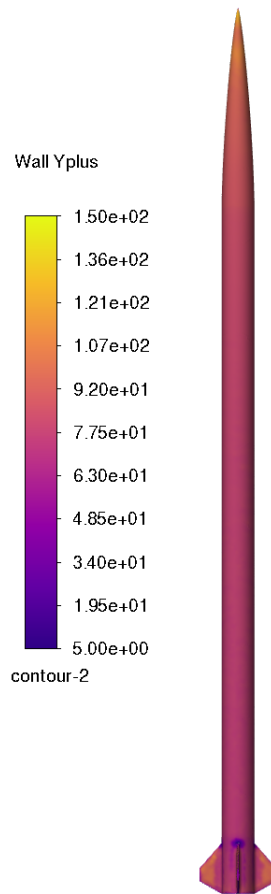


*Figure 32 Y-Plus for Mach 1.05*

A contour of the mass imbalance still left in the solution for the 210 m/s is shown in Figure 33. There is a very low mass imbalance around and upstream of the rocket, which means the solution is very likely to have converged properly.

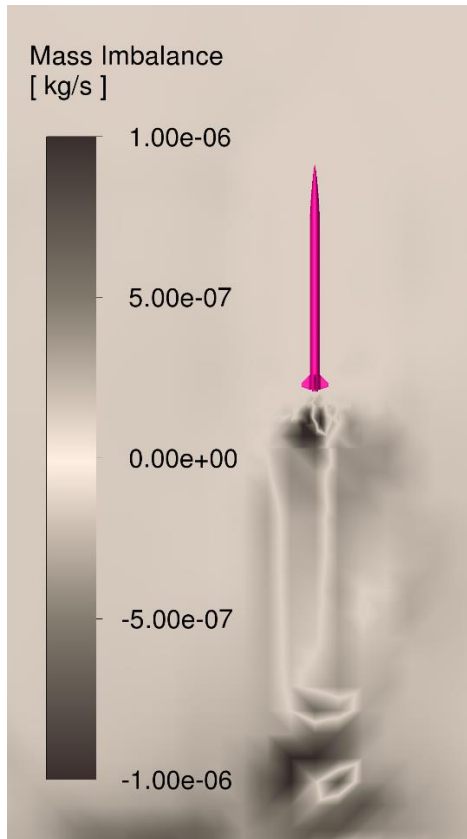


Figure 33 Mass Imbalance in the Solution for 210 m/s

To confirm that the cells are small enough to accurately capture all the relevant flow behavior, each flow region had cases ran with varying max cell size to see if decreasing the maximum element size changes the results significantly. As drag is the primary value of interest it was used as the value of interest in this analysis. The results of this analysis can be seen in Table 3.

Table 3 Analysis Results for Max Side Length and Drag Force

Max Element Side Length (m)	Drag Force (N)
-----------------------------	----------------

0.32	47.784
0.16	47.819
0.08	47.822

Contours of Mach number and static pressure for the Mach 1.05 at angle of attack of 0 can be seen in Figures 34 and 35, and the contours for an angle of attack of 10 can be seen in Figures 36 and 37. 10 was designed to be the highest angle of attack to be used before the pressure far field boundary would start to affect the flow around the rocket significantly. In the bottom right of each of the 10 contours, the effects of the pressure far field boundary can be seen just below the rocket.

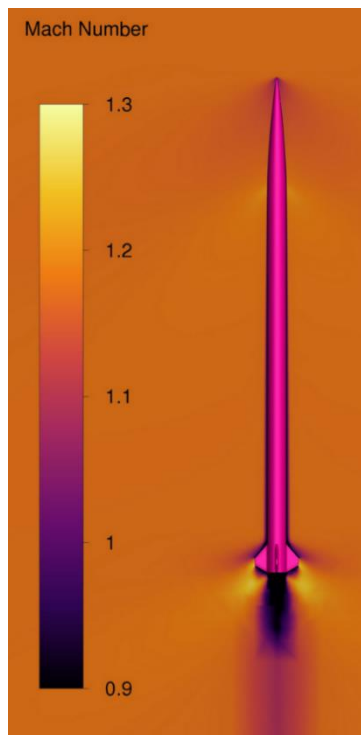
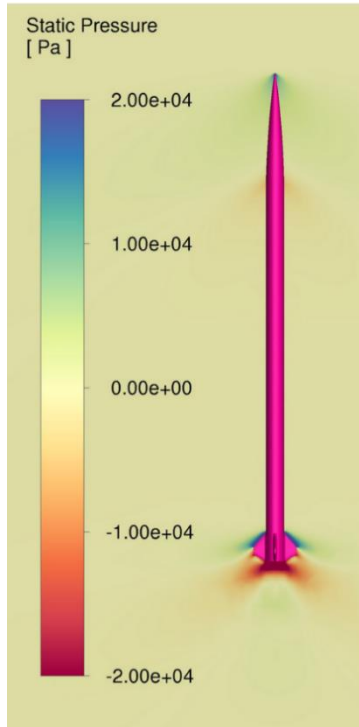


Figure 34 Mach Number Contour for Mach 1.05, Angle of Attack of 0 degrees



*Figure 35 Static Pressure Contour for Mach 1.05, Angle of Attack of 0 degrees*

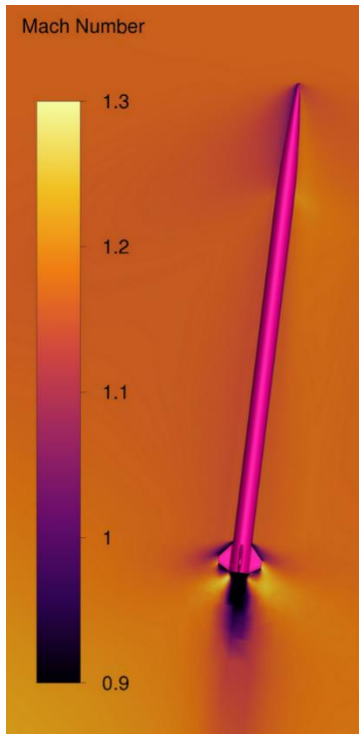


Figure 36 Mach Number Contour for Mach 1.05, Angle of Attack of 10 degrees

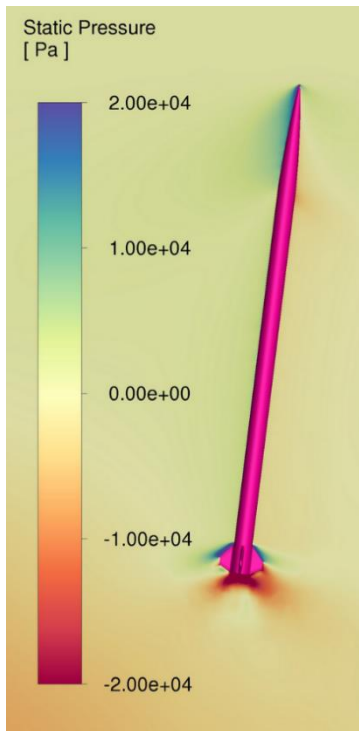


Figure 37 Static Pressure Contour for Mach 1.05, Angle of Attack of 10 degrees

## 4.0 Results

### 4.1 ARS

The ARS subgroup successfully fabricated the fins and assembled the rocket, the completed rocket can be seen in Figure 38.

First the fins were attached to the body using the fin jig and epoxy. Then a layup of 4 layers of carbon fiber was performed onto the fins. After sanding down the body tube and fins, a few layers of primer and spray paint was applied for aesthetics. The team wanted a fun design for the rocket, so bright colors and stickers were used for the design. After the team was satisfied with how the rocket looked, 2 layers of clear coat spray paint were applied to seal everything. Overall, the design was successful because the rocket met the objectives established in section 1 of the report. All internal components fit with ample room if needed.



*Figure 38 Completed Rocket Assembly*

### 4.2 Propulsion, Thermal, and Separation Systems

#### 4.2.1 NASA CEA Analysis

With the previously discussed inputs, NASA CEA was able to output the following parameters. First, seen in Table 4 is the composition of the exhaust gas.



Table 4 Composition of Exhaust Gas

Species	Mole Fraction
ALCL	0.00050
ALCL2	0.00008
ALCL3	0.00007
ALHCL2	0.00001
*ALO	0.00002
ALOCL	0.00012
ALOH	0.00077
ALOHCL	0.00021
ALOHCL2	0.00068
AL(OH)2	0.00012
AL(OH)2CL	0.00042
AL(OH)3	0.00023
*CO	0.24126
*CO2	0.04191
*CL	0.00769
CLO	0.00001
CL2	0.00002
*H	0.01465
HALO2	0.00001
HCO	0.00002

Species	Mole Fraction
HCL	0.14748
HOCL	0.00001
*H2	0.18782
H2O	0.25415
NH3	0.00001
*NO	0.00057
*N2	0.07883
*O	0.00035
*OH	0.00821
*O2	0.00019
AL2O3(L)	0.01354

The products of the reaction listed with an asterisk are deemed notable products by the software. As seen in the table, the largest products of the reaction are H<sub>2</sub>O, CO, and HCL. Desired values used in the COMSOL analysis were calculated in section 3.2.2.

#### 4.2.2 Physics Coupling and Results

The solver that COMSOL uses was unable to find a consistent time dependent solution for the coupled fluid and heat problem. To successfully solve the problem, the time dependent heat transfer solution was coupled with the stationary fluid solution at the end of the propellant burn (0.7s). The parameters of interest were the surface temperature of the motor as well as the fluid flow out of the motor. Figures 40 and 39 respectively show the 2D and 3D temperature

distribution throughout the model, and Figure 41 shows the numerical values plotted as a function of distance from the axis of symmetry of the motor.

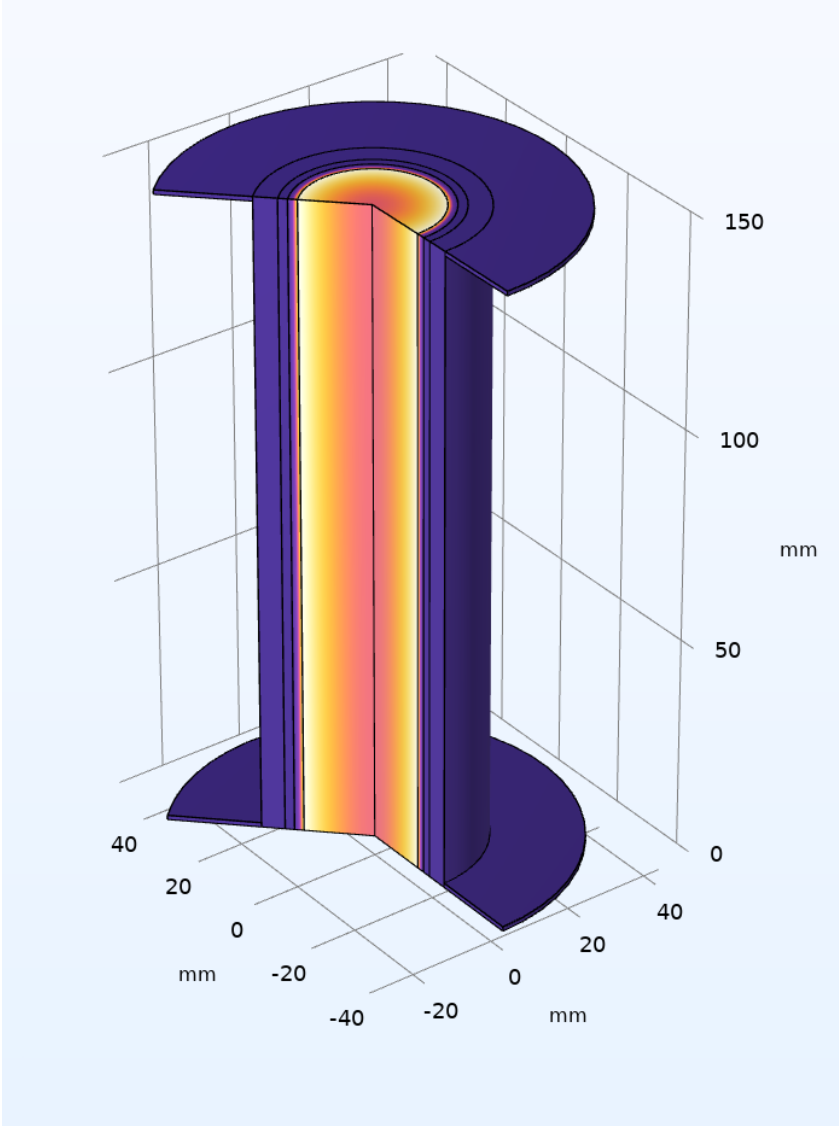


Figure 39 Heat Transfer Distribution

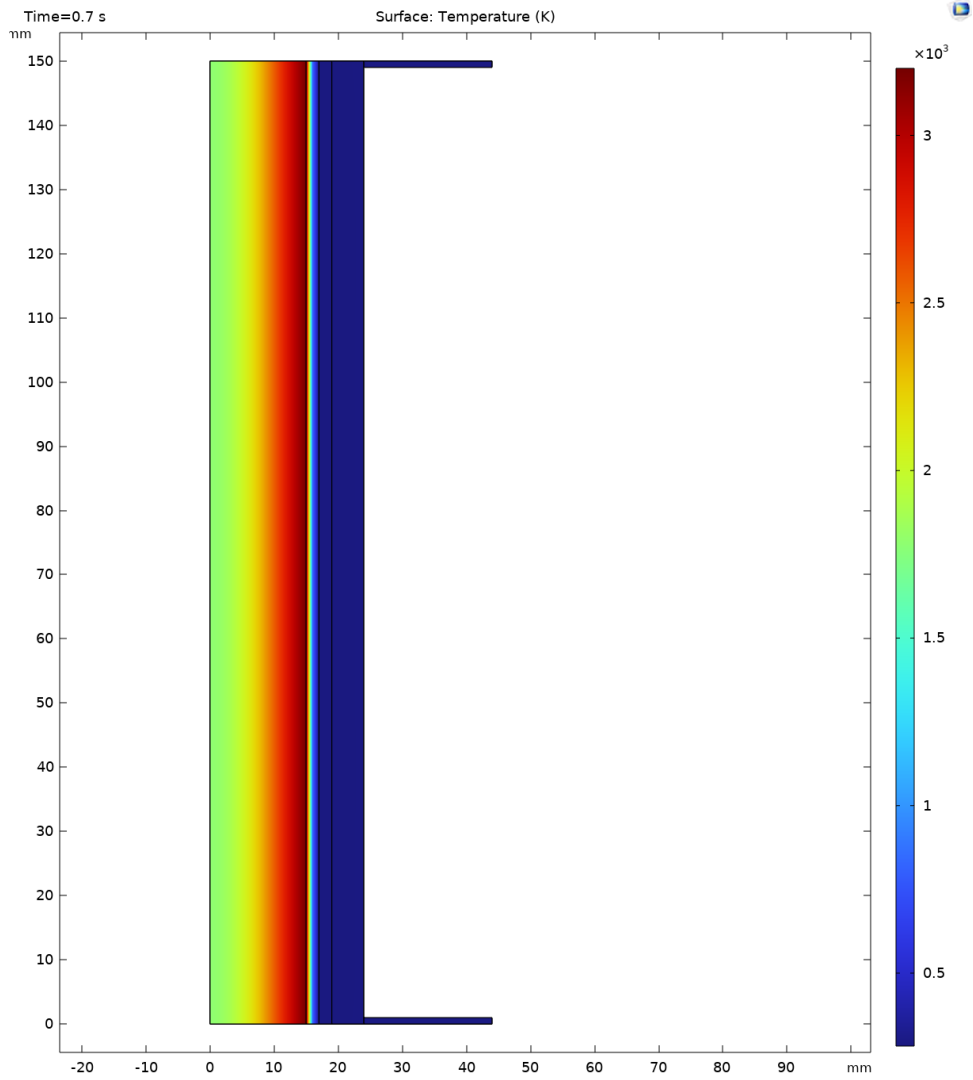
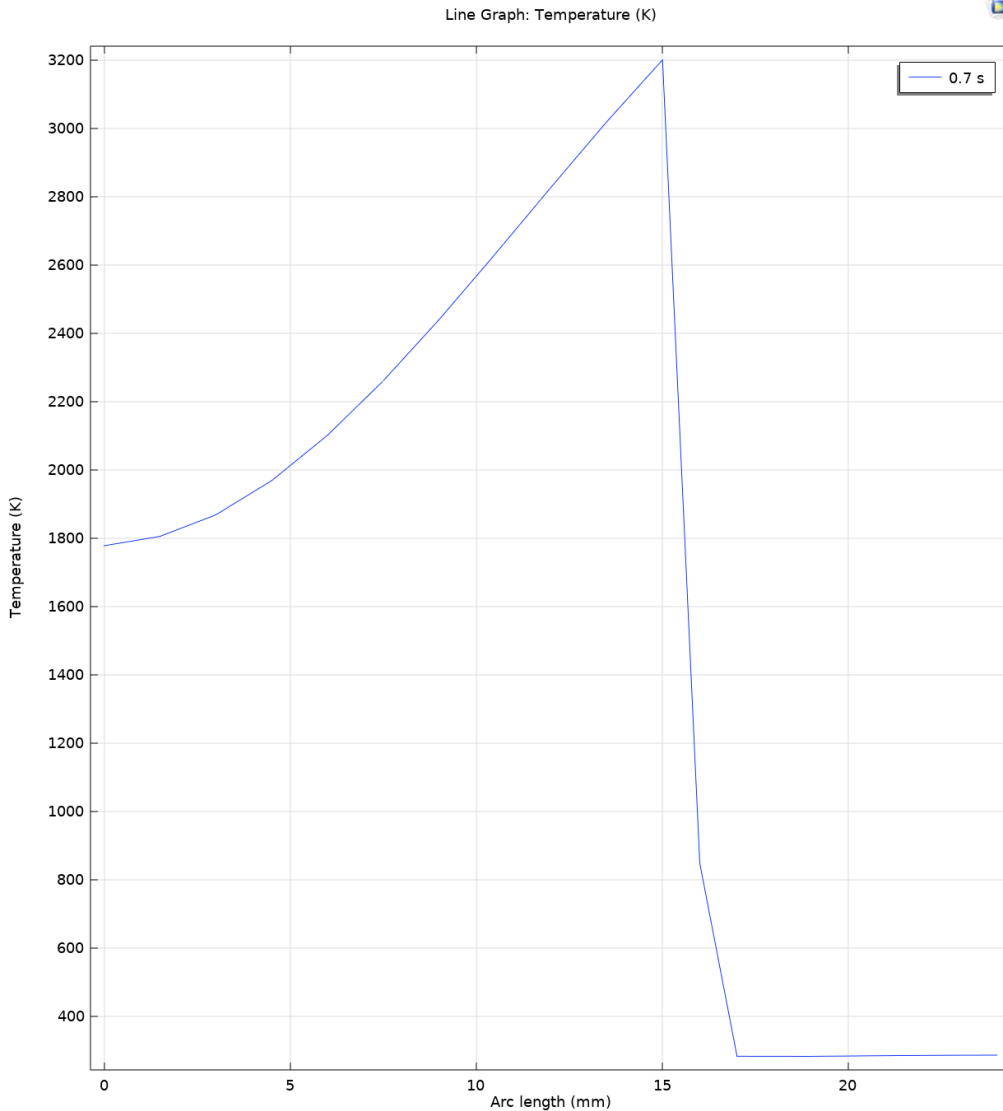


Figure 40 2D Heat Transfer Distribution



*Figure 41 Temperature Distribution Across Motor Assembly*

As seen in Figure 39 on the boundary of the flame zone, there was a temperature defined from the CEA software of 3201 K. The outflow of exhaust gas causes the heat transfer to lessen closer to the axis of symmetry. As seen in the figure, the aluminum casing provides sufficient thermal isolation from the rest of the model. As seen in the figure, the contact of the motor casing and the motor mounting tube does not exceed around 310 K, so there are not going to be

any failure issues due to the thermal loads of the motors. The velocity of the fluid flow can be seen in Figure 42.

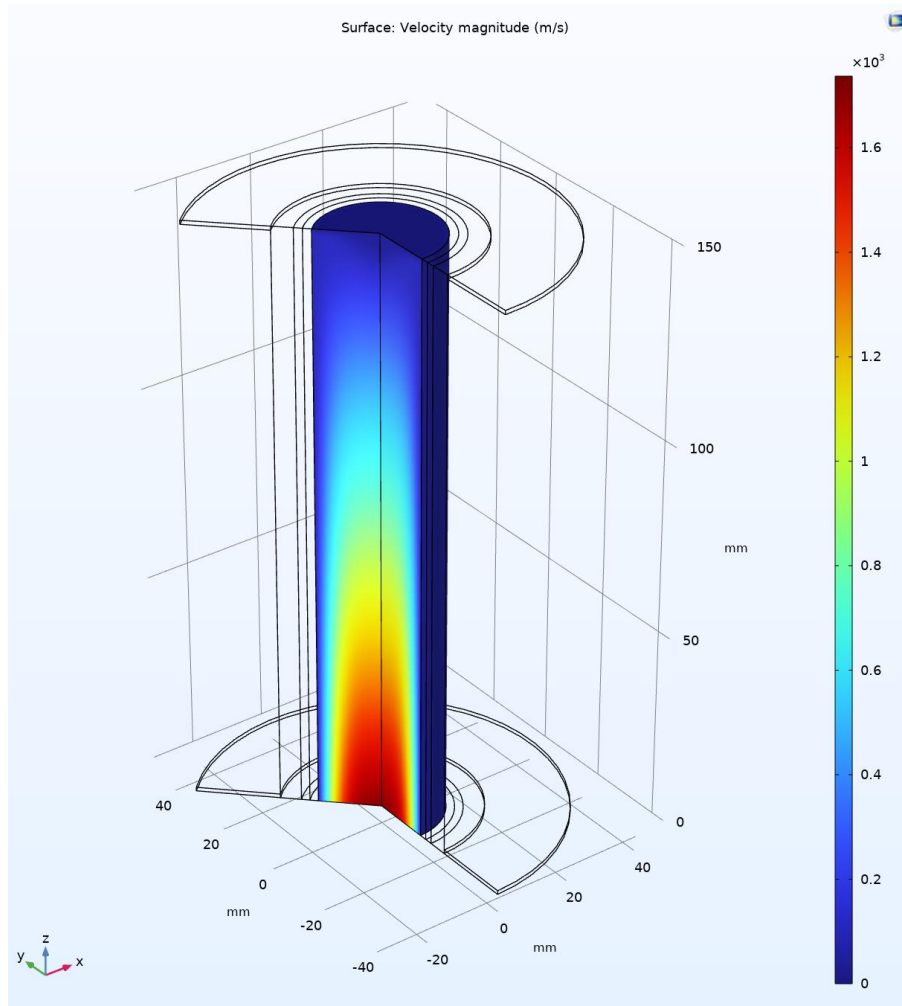


Figure 42 Fluid Velocity in Motor

The peak velocity in the motor reaches about 2000 m/s. Using values from Aerotech and the CEA analysis, the exhaust velocity can be estimated by dividing the thrust by the mass flow rate. According to the manufacturer, the peak thrust of the motor reaches 325N, corresponding to a velocity of around 2300 m/s. This difference in velocity between the manufacturer data and the COMSOL model can be attributed to the nozzle that was omitted in the COMSOL model. The model considers the aft end of the motor to the plane immediately before the nozzle begins.

Nozzle theory determines that the exhaust gas will be accelerated when going through the nozzle. However, the nozzle geometry is not available online, so this could not be included in the model.

#### 4.2.2 Motor Structure Integrity

To test the motor's structural integrity, the PTSS subgroup used ANSYS Mechanical. Simulating the motor design with an applied linear force at the bottom of the motor mount tube enabled the team to examine the range in yield stress and deflection. The input force was 325 Newtons over about 0.7 seconds to replicate the experienced force at takeoff.

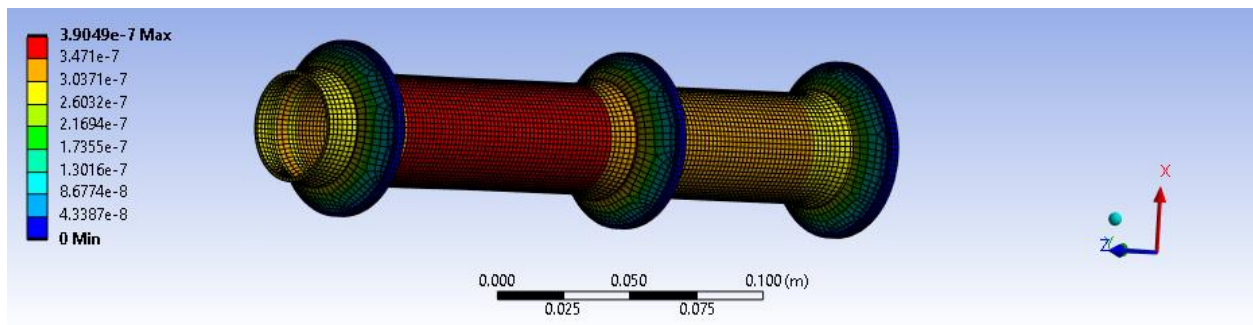


Figure 43 Deflection on Motor Mount, ANSYS Mechanical simulation

The maximum deformation was expected to be 3.9049e-7 meters. This is well within acceptable margins to not cause structural problems for the rocket.

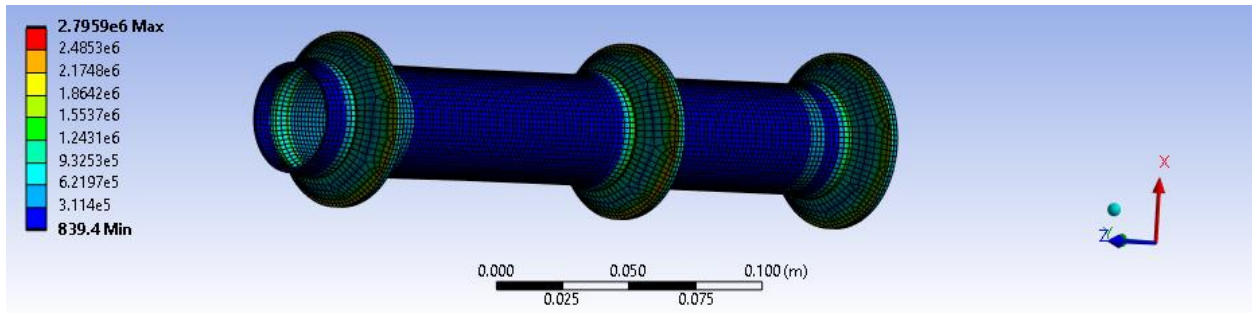


Figure 44 Max Stress on Motor Mount, ANSYS Mechanical simulation

The maximum yield stress was expected to be 2.8 MPa. Since the centering rings were made from plywood with an approximate yield strength of 27.6 MPa, this is within acceptable margins for maintaining structural integrity.

#### 4.2.3 Innovative Design Theory

The innovative design followed the ANSYS Mechanical analysis of a supersonic motor. This motor, the Aerotech J510W would enable the rocket to fly to an altitude exceeding that of the ceiling. Fortunately for the team, the use of this motor would allow the motor mount sizing and assembly to remain the same (38 mm motor mount). The simulation was developed in OpenRocket to select this motor. Then, the same motor mount assembly was input into ANSYS Mechanical with an applied force of 1041.7 N over a span of 0.7 seconds.

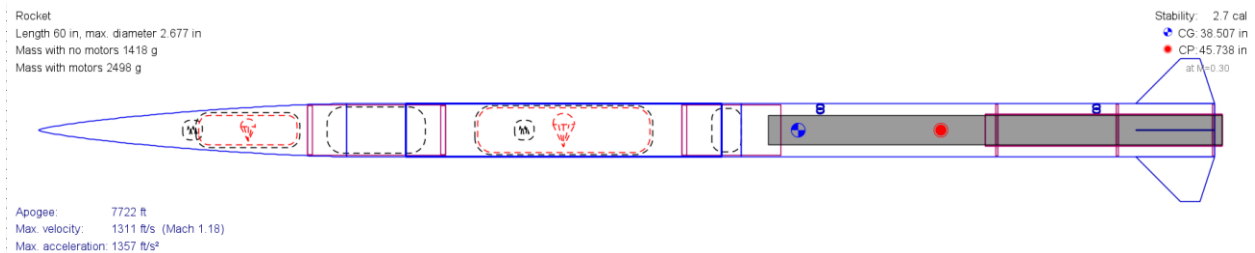


Figure 45 Supersonic Solution, OpenRocket Simulation



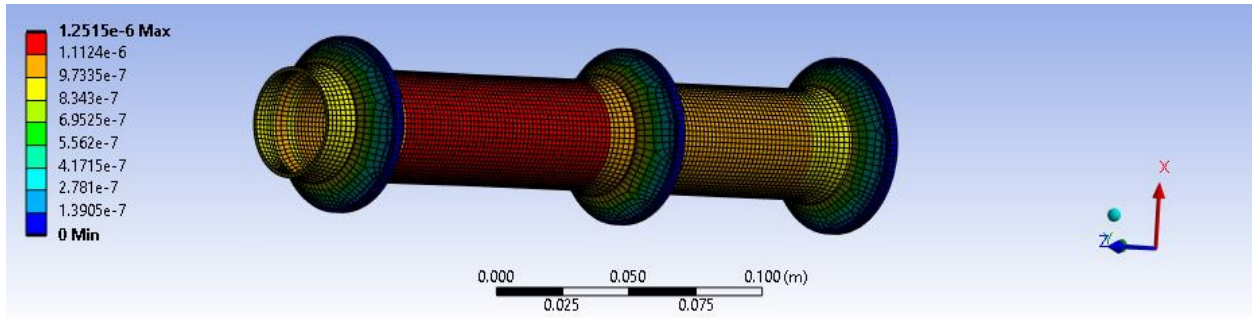


Figure 46 Deflection on Motor Mount, Supersonic

Given the fact that the materials of the 38 mm motor mount remain the same between the original and supersonic models, even with the maximum deflection being approximately  $1.2515 \times 10^{-6}$  meters, this is well within the acceptable range for the assembly's structural integrity.

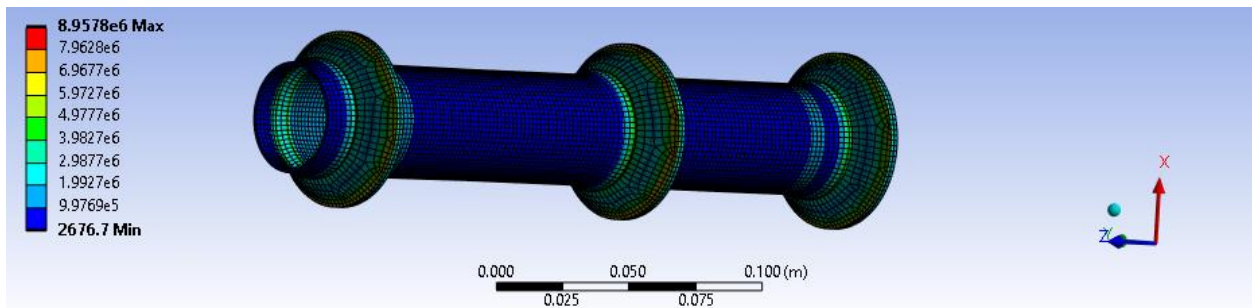


Figure 47 Max Stress on Motor Mount, Supersonic

Furthermore, the max stress on the motor mount, approximately 8.9578 MPa, may be sufficiently tolerated by the plywood centering rings, at which most of the stress is focused. Therefore, the plausibility of this innovative solution's successful implementation is high. Fortunately, although this supersonic capability is beyond the scope of this project, using this motor would enable the team to reach an additional feat in terms of altitude. This would also

allow the team to maximize altitude with the total weight of the rocket. Namely, in terms of the propulsion subsystem, the motor mount would not need to be changed to accommodate this ambitious motor, thereby conserving costs relative to increased capability.

### 4.3 Flight Dynamics Analysis

#### 4.3.1 Fin Sim Analysis

FinSim uses two main methods to calculate the divergence and flutter velocity: the Theodorsen method and the U vs G method. The Theodorsen method is a of calculating the pressure around an airfoil using a Fourier transform to an impulsive incident [FinSim]. Using the Theodorsen method, the results were determined as in Figure 48.

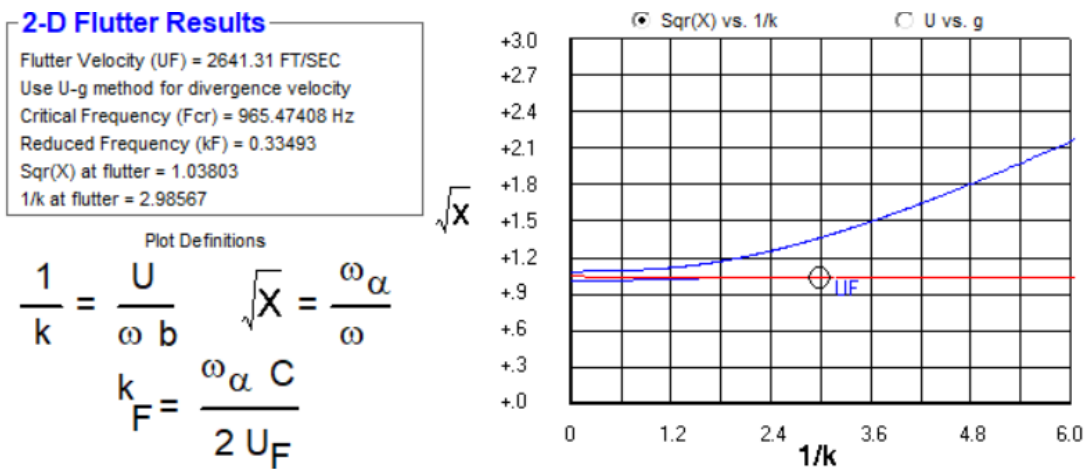


Figure 48 FinSim Theodorsen Calculations for Velocities

Using the Theodorsen method, the calculated flutter velocity was 2641.31 ft/s. However, the team was unable to calculate the divergence velocity using this method. With the U vs G method, the flutter velocity was calculated.

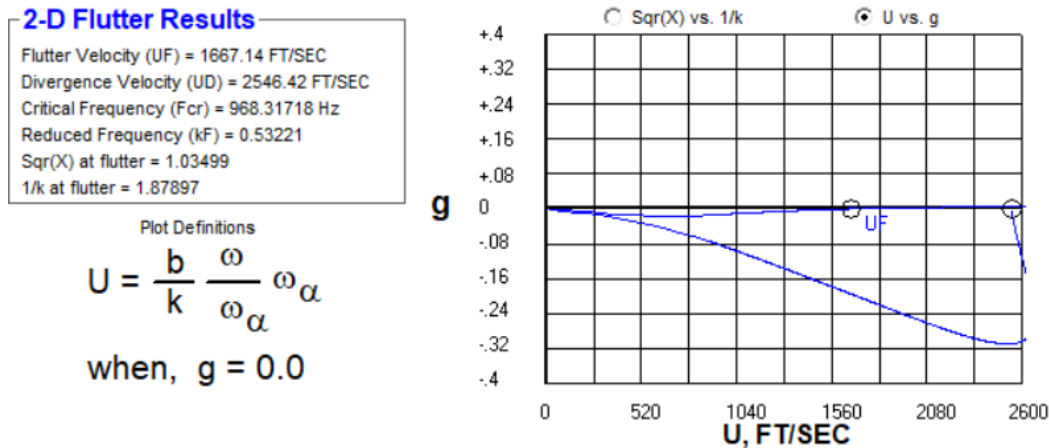


Figure 49 FinSim U-g Calculations for Velocities

Using the U-g method, the calculated flutter velocity was 1667.14 ft/s and the divergence velocity were 2546.42 ft/s. Using the U-g method, the flutter velocity was less than that of the Theodorsen method (about 1000 ft/s smaller). While this velocity is significant, it is still much larger than our predicted maximum velocity of 340 ft/s.

The fin thickness was set to 1/8<sup>th</sup> of an inch and flutter and divergence velocities were computed to determine if thickness was viable. Fin Sim predicted the flutter velocity of 2543.34 ft/s and divergence velocity of 1619.14 ft/s. Given our RASAero predicted max velocity of 1259 ft/s in the supersonic case, the fins can survive both the subsonic and supersonic launches. With 1/4<sup>th</sup> inch fin thickness, our divergence and flutter velocities were 4526.61 ft/s and 71110 ft/s. These velocities are also greater than the projected max velocity but add unnecessary bulkiness

to the fins. The 1/8<sup>th</sup> inch plywood fins are structurally capable of flight and using the 1/4<sup>th</sup> inch would be a waste of resources and power.

#### 4.3.2 6 Degrees of Freedom Simulator Predictions

Using the aerodynamic data from the CFD simulations, a model of the drag can be created. The drag data for 0° roll and 0° angle of attack can be seen in Figure 50.

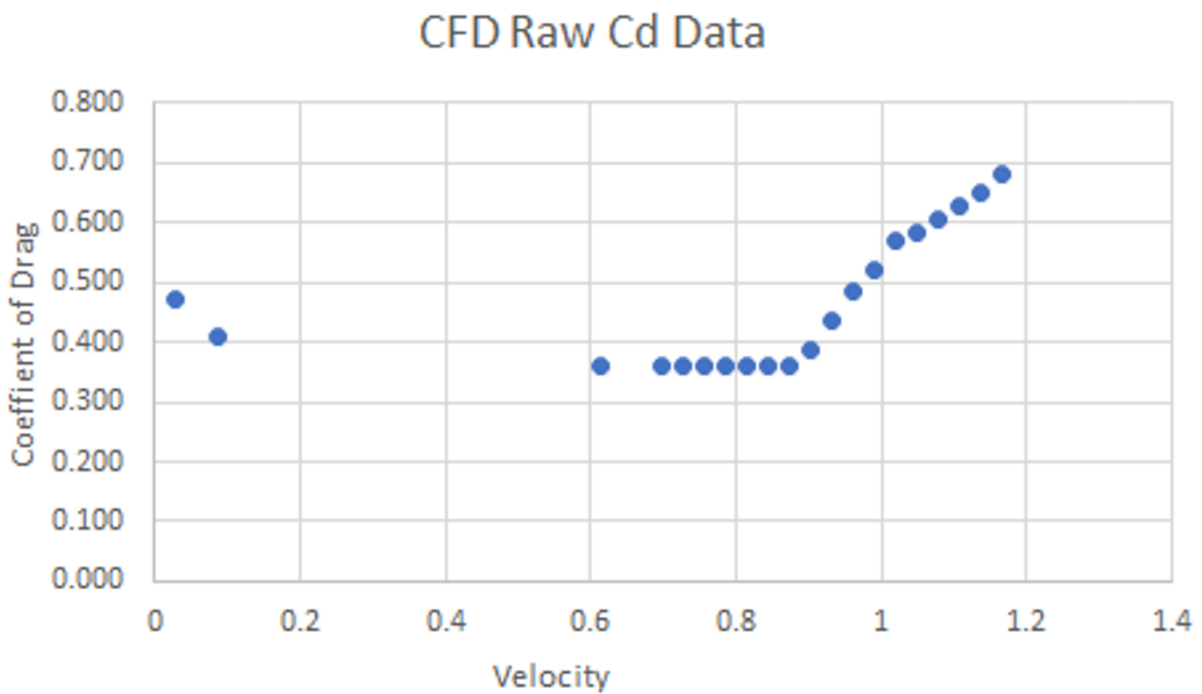


Figure 50 CFD Drag Data

These datapoints alone are not enough to know the aerodynamic forces for our full range of conditions the rocket may experience, a method turning these single points into a continuous

surface must be chosen. For the subsonic region, the force coefficient vs velocity can be modeled with an exponential decay of the form

$$C_f = A + B * C^V \quad (8)$$

This gives the team 36 different curves for the various force coefficients, angle of attacks, and rolls for the subsonic region. The drag coefficient curve for 0° roll and 0° angle of attack can be seen in the first part of Figure 51 up to Mach 0.7 and is compared against RASAero's data. The rest of the gaps in the data can now be linearized to cover the rest of the flow conditions.

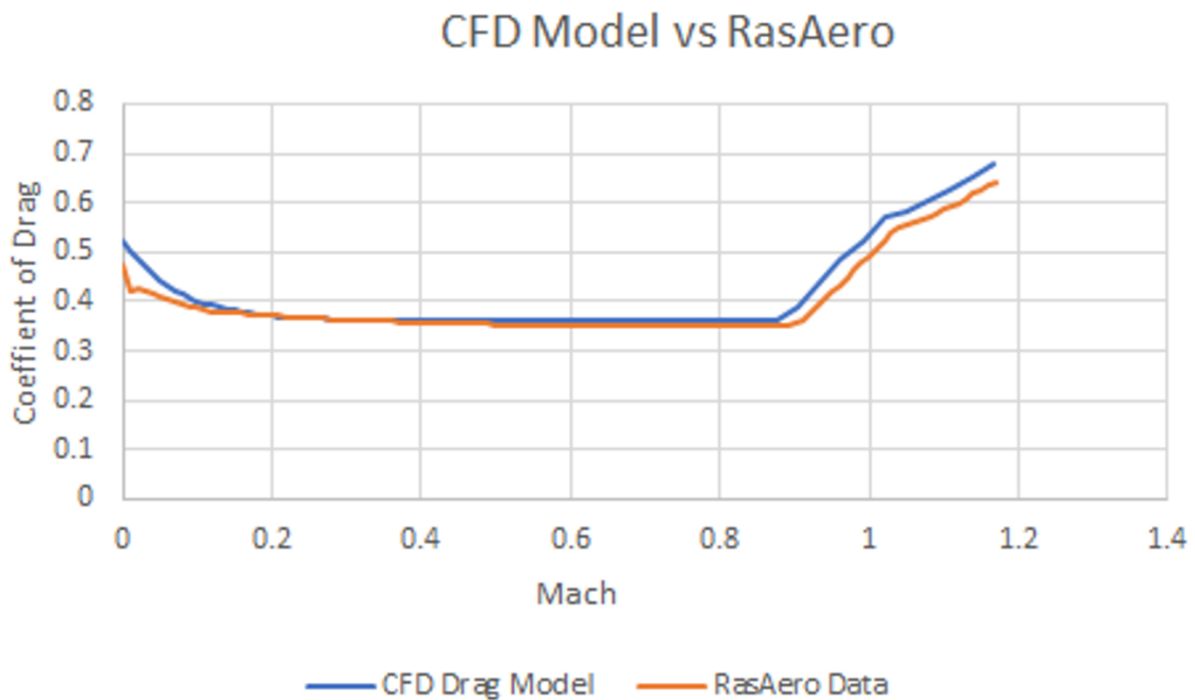


Figure 51 CFD Drag Model versus RASAero

The full aerodynamic model of the rocket can now be inputted into the 6DOF, and the flight can be modeled. A flight with no wind at a 0° launch angle was used to compare the results of

the 6DOF to OpenRocket. The 6DOF estimated apogee to be around 1688 ft compared to the 1610 ft found from OpenRocket. The plots of altitude and total velocity vs time of both simulations can be seen in Figures 52 and 53.

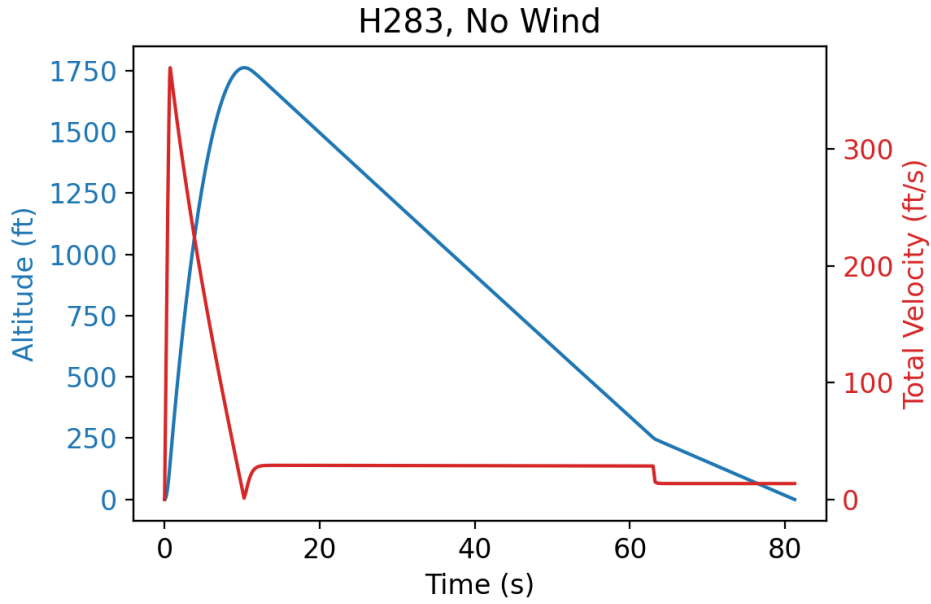


Figure 52 Altitude and Velocity versus Time, 6DOF

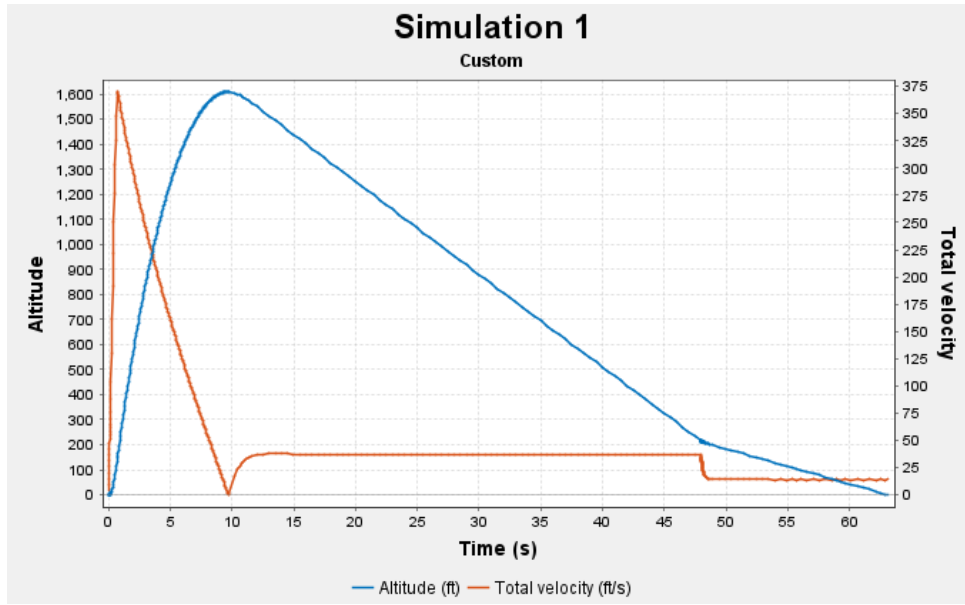


Figure 53 Altitude and Velocity versus Time, OpenRocket

#### 4.3.3 Sled Design

The design of the sled is very simple with two slots on either side, one for a battery and one for a sensor. Since the sizes of the two sensors are different, one side can only fit the TeleMega, and the other can only fit the RRC3. The slot sizes were created to snugly fit the sensors and the batteries to help keep them secure during the launch. Figure 15 shows the complete sled, with the sensors and batteries wired as depicted in the wiring diagram in Figure 12.

## 5 Conclusions and Recommendations

### 5.1 Airframe Recovery System

The ARS subgroup designed and fabricated the airframe utilizing SolidWorks and OpenRocket to model the airframe and visualize for weight allocations and stability

requirements. Additionally, the subgroup lead the integration of all components of the airframe including the payload, the motor and motor mount, recovery system and sensors and gyros. The subgroup also designed the baseline recovery system and researched and analyzed an innovative recovery system. For future projects, the subgroup recommends the following:

1. Determine all materials needed for the airframe itself within the first term and make a list with links for purchasing as early as possible to minimize shipping or stocking issues. Additionally, always have a backup or two for each item.
2. Prioritize the fins and the layups. To be able to feel confident in applying a layup, be it fiberglass or carbon fiber, at least a few practice cans should be performed, and this requires having a fin jig, standoffs, the mesh for the overlay, and epoxy. The layup takes at least two days if the room the epoxy cures in is very warm, and longer if the room is cold so materials for this need to be prioritized in purchasing.
3. Prioritize the baseline rocket. The innovative design, while still needing time and attention, can be put lower on the priority list as having a baseline rocket that is ready to launch is ultimately more important. With this recommendation, refresh your CAD modeling skills as it is important for not just the ARS team's use but for all subgroups to have access to a good model.

## 5.2 Propulsion, Thermal and Separation System

Throughout the project duration, the PTSS subgroup analyzed thermodynamic loads on the rocket motor mount assembly using COMSOL. The subgroup additionally examined the theoretical structural integrity of the mount assembly using ANSYS Mechanical with an applied maximum thrust from the motor manufacturer, Aerotech. The subgroup explored an innovative supersonic motor solution which would enable a flight to reach a higher altitude at no risk to the



structural integrity of the rocket and the motor mount assembly. Furthermore, the modelled and purchased motor mount would not need to be altered, thereby preserving project costs. For future projects, some recommendations would be to:

1. Analyze the thermal distribution of the fluid flow out of the nozzle using COMSOL and simulate the effect of different nozzle materials.
2. Prioritize finalizing an OpenRocket design early into the project's timeline so a motor can quickly be selected. This mostly involved issues with internal communication and the use of multiple OpenRocket simulations.
3. Prioritize the mainstream rocket. This will provide additional time to focus on an innovative design.

### 5.3 Flight Dynamics Analysis

The FDA subgroup successfully analyzed aerodynamic loads across the rocket and simulated the rocket's flight trajectory. Additionally, the subgroup designed a sled for the TeleMega and RRC3 sensors and assisted in the construction and assembly of the rocket. For future MQPs, some recommendations would be:

1. Expand the 6DOF simulator to better account for changing atmospheric conditions and allow the use of simplified drag models so it can replace OpenRocket for the design phase.
2. Find or create external software outside of FinSim for structural analysis of fins.

## 5.4 Broader Impacts

The general interest in high power model rocketry is not likely to decrease in upcoming years (Witze, Alexandra, 2023). As more individuals are exploring the areas of science, technology, engineering, and math (STEM), they may deem model rocketry a positive and engaging method of implementing their knowledge. The research performed during the duration of this project inspired the team to expand their knowledge of various software, machine tooling, and engineering and scientific principles. The project also allowed its members to physically engage with the construction of the final mainstream rocket.

A goal for eventual flight is to safely remain within the site's bounds to neither damage property and natural resources, nor pollute the area. In effectively predicting and modelling the flight dynamics and selecting an appropriate motor, the team aims to prevent these negative effects upon launch.

## References

Adde, Yeshurun (Kibret) & Lulseged, G. (2020). Design of a Solid Rocket Propulsion System.

10.13140/RG.2.2.11864.93446.

*AeroFinSim description page*. (n.d.). Retrieved February 26, 2024, from

<https://www.aerorocket.com/FinSim.html>

Ansys. (n.d.). Ansys Fluent 12.0 theory guide.

[https://www.afs.enea.it/project/neptunius/docs/fluent/html/th/main\\_pre.htm](https://www.afs.enea.it/project/neptunius/docs/fluent/html/th/main_pre.htm)

Apogee Components, I. (n.d.). Standard Engine Hooks. Model Rockets & How-To Rocketry Information.

[https://www.apogeerockets.com/Building\\_Supplies/Motor\\_Retainers\\_Hooks/Engine\\_Hooks/Standard\\_Engine\\_Hooks](https://www.apogeerockets.com/Building_Supplies/Motor_Retainers_Hooks/Engine_Hooks/Standard_Engine_Hooks)

Apogee Components, I. (n.d.-a). Motor Retention. Apogee Rockets.

[https://www.apogeerockets.com/How-To/Motor\\_Retention](https://www.apogeerockets.com/How-To/Motor_Retention)

Cipolla, John. "AeroRocket - FinSim {software}." Rocket Reviews,

[www.rocketreviews.com/aerorocket-FinSim-by-john-champion.html](http://www.rocketreviews.com/aerorocket-FinSim-by-john-champion.html). Accessed 6 Oct.

2023.

David G. Goodwin, Harry K. Moffat, Ingmar Schoegl, Raymond L. Speth, and Bryan W. Weber.

Cantera: An object-oriented software toolkit for chemical kinetics, thermodynamics, and transport processes. <https://www.cantera.org>, 2023. Version 3.0.0.

doi:10.5281/zenodo.8137090

Engine Mounts. Estes Rockets. (n.d.). <https://estesrockets.com/search?q=engine%2Bmount&options%5Bprefix%5D=last>

Experimental Sounding Rocket Association. (n.d.). Spaceport America Cup Design, Test, and Evaluation Guide. [https://www.soundingrocket.org/uploads/9/0/6/4/9064598/2023-sa\\_cup\\_dteg\\_v2.2.9\\_10-24-23.pdf](https://www.soundingrocket.org/uploads/9/0/6/4/9064598/2023-sa_cup_dteg_v2.2.9_10-24-23.pdf)

Fallon, Brandon, and MIT. "APCP Solid Propulsion Development." *APCP Solid Propulsion Development*, 11 Sept. 2021, [brandonfallon.com/apcp-solid-propulsion-development/](http://brandonfallon.com/apcp-solid-propulsion-development/).

Hansen, J., & Loftin, L. K. (1987). Quest for Performance: The evolution of modern aircraft. *Technology and Culture*, 28(3), 734. <https://doi.org/10.2307/3105034>

Inc, A. C. (n.d.). *Motor retention : Apogee Rockets, Model Rocketry Excitement starts here.* [https://www.apogeerockets.com/How-To/Motor\\_Retention](https://www.apogeerockets.com/How-To/Motor_Retention)

Krech, Bob. (2011, August 14). Landing Speed [Msg 4]. The Rocketry Forum, <https://www.rocketryforum.com/threads/landing-speed.25383/>

Model rocket safety code - national association of rocketry. NAR. (2022, September 19). <https://www.nar.org/safety-information/model-rocket-safety-code/>

National Association of Rocketry. (2014, June 20). Standard Motor Codes - National Association of Rocketry. National Association of Rocketry - NAR. <https://www.nar.org/standards-and-testing-committee/standard-motor-codes/>

NASA. (n.d.). NASA thermo build (beta). NASA. <https://cearun.grc.nasa.gov/ThermoBuild/>

NASA, (2021). Liquid Rocket Engine. NASA. <https://www.grc.nasa.gov/www/k-12/airplane/rockth.html>

NASA, (2021). Model Rocket Engine. NASA. <https://www.grc.nasa.gov/WWW/k-12/rocket/rktengine.html>

NASA, (2021). Rocket Engine Performance. <https://www.grc.nasa.gov/WWW/K-12/rocket/rktengperf.html>

OpenRocket. OpenRocket Simulator. (n.d.). <https://OpenRocket.info/>

[ *Resources / Aerodynamics for students.* (n.d.).

<http://www.aerodynamics4students.com/aeroelasticity/#:~:text=In%20this%20case%20the%20moment,operating%20speeds%20of%20the%20vehicle>

Stine GH, Stine B. Handbook of Model Rocketry. 7th ed. Wiley; 2004.

Sutton, G. P., & Biblarz, O. (2017). Rocket Propulsion Elements (9th ed.). Wiley.

Van Milligan, T. (n.d.). How to Design and Build Engine Mounts. Apogee Rockets.

<https://www.apogeerockets.com/education/downloads/Newsletter104.pdf>

Witze, Alexandra. “2022 Was a Record Year for Space Launches.” Nature News, Nature

Publishing Group, 11 Jan. 2023, <https://www.nature.com/articles/d41586-023-00048-7>.